Search for Z gamma resonances using leptonic and hadronic final states in proton-proton collisions at root s=13 TeV

The CMS collaboration

2018-09-26

The CMS Collaboration , Sirunyan , A M , Eerola , P , Kirschenmann , H , Pekkanen , J , Voutilainen , M , Havukainen , J , Heikkilä , J K , Järvinen , T , Karimäki , V , Kinnunen , R , Lampén , T , Lassila-Perini , K , Laurila , S , Lehti , S , Lindén , T , Luukka , P , Siikonen , H , Tuominen , E , Tuominiemi , J & Tuuva , T 2018 , ' Search for Z gamma resonances using leptonic and hadronic final states in proton-proton collisions at root s=13 TeV ' , Journal of High Energy Physics , vol. 2018 , no. 9 , 148 . https://doi.org/10.1007/JHEP09(2018)148

http://hdl.handle.net/10138/253497
https://doi.org/10.1007/JHEP09(2018)148

Published for SISSA by Springer

Received: December 8, 2017
Revised: September 3, 2018
Accepted: September 10, 2018
Published: September 26, 2018

Search for Zγ resonances using leptonic and hadronic final states in proton-proton collisions at $\sqrt{s} = 13$ TeV

The CMS collaboration

E-mail: cms-publication-committee-chair@cern.ch

Abstract: A search is presented for resonances decaying to a Z boson and a photon. The analysis is based on data from proton-proton collisions at a center-of-mass energy of 13 TeV, corresponding to an integrated luminosity of 35.9 fb^{-1}, and collected with the CMS detector at the LHC in 2016. Two decay modes of the Z boson are investigated. In the leptonic channels, the Z boson candidates are reconstructed using electron or muon pairs. In the hadronic channels, they are identified using a large-radius jet, containing either light-quark or b quark decay products of the Z boson, via jet substructure and advanced b quark tagging techniques. The results from these channels are combined and interpreted in terms of upper limits on the product of the production cross section and the branching fraction to Zγ for narrow and broad spin-0 resonances with masses between 0.35 and 4.0 TeV, providing thereby the most stringent limits on such resonances.

Keywords: Beyond Standard Model, Hadron-Hadron scattering (experiments), Particle and resonance production

ArXiv ePrint: 1712.03143

https://doi.org/10.1007/JHEP09(2018)148

JHEP09(2018)148

Contents

JHEP09(2018)148

1 Introduction

One of the key aspects of the CERN LHC physics program is the search for new resonances predicted in theories beyond the standard model (SM). Given the fairly stringent limits already set on masses of such resonances in fermionic decay channels (e.g., via dilepton or dijet searches), it is particularly interesting to explore bosonic decay channels, which can dominate if the couplings of a new resonance to fermions are suppressed. Examples of such signatures are decays into a pair of massive bosons: VV and VH, where V represents either a W or a Z boson, and H refers to the recently discovered Higgs boson [1–3]. The latest results from these searches at the LHC are described in refs. [4–15] for the VV channels and in refs. [10, 16–21] for the VH channels.

Diboson decays involving photons, i.e., Wγ, Zγ, and $\gamma\gamma$ channels, are also important, as the search in the $\gamma\gamma$ channel demonstrated by contributing significantly to the discovery of the Higgs boson by the ATLAS and CMS Collaborations in 2012 [1–3]. While a resonance decaying to diphotons cannot be a vector or an axial vector, due to the Landau-Yang theorem [22, 23], having one of the two bosons massive alleviates this constraint. Thus, charged (neutral) bosons of spin 0, 1, or 2 can be sought in the Wγ (Zγ) channel, leading to a broad search program. Such resonances are predicted in many extensions of the SM,

such as technicolor [24] and little Higgs [25] models, as well as models with an extended Higgs boson sector [26, 27] or with extra spatial dimensions [28, 29].

In this paper, we describe a search for $Z\gamma$ resonances in the leptonic ($\ell\ell$, where ℓ refers to e or μ) and hadronic decay channels of the Z boson, as well as the combination of these channels. While the results in this paper are interpreted in terms of spin-0 resonances, they are broadly applicable to spin-1 and spin-2 states, as the signal acceptance depends only weakly on the spin of the resonance [30]. Similar searches in a combination of leptonic and hadronic decay channels of the Z boson have been recently published by ATLAS [31] at $\sqrt{s} = 13\,\text{TeV}$ and by CMS at $\sqrt{s} = 8$ and $13\,\text{TeV}$ [32], based on significantly smaller integrated luminosities. Other searches for $Z\gamma$ resonances have been performed only in the dilepton channels. These include searches by the L3 Collaboration at the CERN LEP [33] and the D0 Collaboration at the Fermilab Tevatron [34, 35]. At the LHC, they have been done by ATLAS at $\sqrt{s} = 7$, 8, and $13\,\text{TeV}$ [30, 36, 37], and CMS at $\sqrt{s} = 8$ and $13\,\text{TeV}$ [38], as well as by ATLAS and CMS using the combined 7 and 8 TeV data [39, 40], and by ATLAS using the $13\,\text{TeV}$ data [30] in the context of a search for the $H \to Z\gamma$ decay.

The present search is for a resonance with a relatively narrow width appearing as an excess over the smooth $Z\gamma$ invariant mass ($m_{Z\gamma}$) spectrum constructed from an energetic photon and the $Z \to \ell\ell$ or $Z \to q\bar{q}$ decay products. While a search in the leptonic channels has lower SM backgrounds, resulting in higher sensitivity to resonance masses $<1\,\text{TeV}$, at larger mass values, where backgrounds are small, the hadronic channels, with their higher branching fraction, dominate the sensitivity. The backgrounds in both channels are determined directly from fits to data.

The Z boson decays in the leptonic channels are reconstructed using an electron or a muon pair. The dominant backgrounds in the $\ell\ell\gamma$ channel are the irreducible contribution from continuum $Z\gamma$ production and the reducible backgrounds from either final-state radiation in $Z \to \ell\ell$ events or from Z boson production in association with one or more jets (Z+jets), where a jet is misidentified as a photon.

The Z boson decay products in the hadronic channels can be reconstructed either as two well-separated small-radius jets, or as a single large-radius jet (J) resulting from the merging of the two quark jets because of the large Lorentz boost of a Z boson produced in the decay of a heavy resonance. The fraction of events corresponding to the merged topology, which has low background from SM sources, increases with the mass of the resonance. To optimize signal relative to background, in this paper we consider just the merged jet topology ($J\gamma$), and thus the search in the hadronic channels is focused on relatively high resonance masses where the trigger for these events is efficient. We use jet substructure techniques to infer the presence of two subjets, and dedicated b tagging algorithms to identify those subjets that originate from b quark fragmentation. This provides the means to distinguish a signal from the dominant background from prompt-photon and QCD multijet production, with one of the jets spuriously passing jet substructure requirements (and, in the latter case, with another jet mimicking a photon).

JHEP09(2018)148

2 The CMS detector

The central feature of the CMS apparatus is a superconducting solenoid of 6 m internal diameter, providing a magnetic field of 3.8 T. Within the solenoid volume are a silicon pixel and strip tracker, a lead tungstate crystal electromagnetic calorimeter (ECAL), and a brass and scintillator hadron calorimeter (HCAL), each composed of a barrel and two endcap sections. Forward calorimeters extend the pseudorapidity coverage provided by the barrel and endcap detectors. Muons are detected in gas-ionization chambers embedded in the steel flux-return yoke outside the solenoid.

The silicon tracker measures charged particles within the pseudorapidity range $|\eta| < 2.5$. It consists of 1440 silicon pixel and 15 148 silicon strip detector modules. For nonisolated particles of $1 < p_T < 10$ GeV and $|\eta| < 1.4$, the track resolutions are typically 1.5% in p_T and 25–90 (45–150) μm in the transverse (longitudinal) impact parameter [41]

The ECAL consists of 75 848 lead tungstate crystals, which provide coverage in pseudorapidity $|\eta| < 1.48$ in a barrel region (EB) and $1.48 < |\eta| < 3.0$ in two endcap regions (EE). Preshower detectors consisting of two planes of silicon sensors interleaved with a total of $3X_0$ of lead are located in front of each EE detector.

In the region $|\eta| < 1.74$, the HCAL cells have widths of 0.087 in pseudorapidity and 0.087 in azimuth (ϕ). In the η-ϕ plane, and for $|\eta| < 1.48$, the HCAL cells map on to 5×5 arrays of ECAL crystals to form calorimeter towers projecting radially outwards from close to the nominal interaction point. For $|\eta| > 1.74$, the coverage of the towers increases progressively to a maximum of 0.174 in $\Delta\eta$ and $\Delta\phi$. Within each tower, the energy deposits in ECAL and HCAL cells are summed to define the calorimeter tower energies, subsequently used to provide the energies and directions of hadronic jets.

The electron momentum is estimated by combining the energy measurement in the ECAL with the momentum measurement in the tracker. The momentum resolution for electrons with $p_T \approx 45$ GeV from $Z \to ee$ decays ranges from 1.7% for nonshowering electrons in the barrel region to 4.5% for showering electrons in the endcaps [42].

Muons are measured in the pseudorapidity range $|\eta| < 2.4$, with detection planes made using three technologies: drift tubes, cathode strip chambers, and resistive-plate chambers. Matching muons to tracks measured in the silicon tracker results in a relative transverse momentum resolution for muons with $20 < p_T < 100$ GeV of 1.3–2.0% in the barrel and better than 6% in the endcaps. The p_T resolution in the barrel is better than 10% for muons with p_T up to 1 TeV [43].

Events of interest are selected using a two-tiered trigger system [44]. The first level, composed of custom hardware processors, uses information from the calorimeters and muon detectors to select events at a rate of around 100 kHz within a time interval of less than 4 μs. The second level, known as the high-level trigger, consists of a farm of processors running a version of the full event reconstruction software optimized for fast processing, and reduces the event rate to around 1 kHz before data storage.

A more detailed description of the CMS detector, together with a definition of the coordinate system used and the relevant kinematic variables, can be found in ref. [45].

JHEP09(2018)148

3 Data sets and event selection

The data used in this search correspond to an integrated luminosity of 35.9 fb^{-1} recorded by the CMS experiment at $\sqrt{s} = 13\,\text{TeV}$ in 2016. The high instantaneous luminosity delivered by the LHC results in additional interactions in the same or neighboring bunch crossings (pileup) as the hard scattering interaction. The average number of pileup interactions in the 2016 data set is around 23.

In the eeγ channel, the selected events are required to pass a double-photon trigger with the transverse momentum $p_\text{T} > 60\,\text{GeV}$ and pseudorapidity $|\eta| < 2.5$ requirements on both photon candidates. Since the photon trigger requirements do not include any track veto, this trigger is equally efficient in selecting photon and electron candidates. A combination of single-muon triggers requiring $p_\text{T} > 50\,\text{GeV}$ and $|\eta| < 2.4$ on a muon candidate are used in the $\mu\mu\gamma$ channel. In the Jγ channel, we require a logical "OR" of several triggers with the separate requirements: the scalar sum of transverse energies of all reconstructed jets (H_T) is above 800 or 900 GeV; a jet is present with the transverse energy above 500 GeV; and a photon candidate is present with $p_\text{T} > 165$ or 175 GeV and $|\eta| < 2.5$. We determine the selection efficiency for these trigger combinations using unbiased data samples collected with different triggers. The triggers are found to be 98–100% efficient with respect to the offline selection, for the entire mass range used, in all three channels. The small residual inefficiency is taken into account when calculating the signal acceptance.

Simulated signal events of spin-0 resonances decaying to Zγ are generated at leading order (LO) in perturbative QCD using PYTHIA 8.205 [46] with the CUETP8M1 [47, 48] underlying-event tune. Several samples are generated with masses ranging from 0.3 to 4.0 TeV. Two resonance width assumptions were used in the simulation: one, termed "narrow", has its width (Γ_X) set to 0.014% of the resonance mass (m_X), and the second, referred to as "broad", has $\Gamma_\text{X}/m_\text{X} = 5.6\%$. The first choice corresponds to a resonance with a natural width much smaller than the detector resolution. The second choice facilitates a direct comparison with the previous CMS publications [32, 38]. We assume no interference between signal and the SM nonresonant Zγ production.

Simulated background events do not enter the analyses directly, as the backgrounds are obtained from fits to data, but are used to assess the accuracy of the background model and to optimize event selection. Standard model nonresonant Z($\ell\ell$)γ production, which is expected to be the dominant background process in the $\ell\ell\gamma$ channel, is generated at next-to-leading order (NLO) accuracy using the MADGRAPH5_aMC@NLO 2.3.3 generator [49, 50]. The Z($\ell\ell$)+jets events with a jet misidentified as a photon, which constitute a subdominant source of background, are generated at LO using MADGRAPH5_aMC@NLO, as are the dominant γ+jets and QCD multijet events, as well as subdominant hadronically decaying W+jets and Z+jets backgrounds in the Jγ channel. All background events are processed with PYTHIA for the description of fragmentation and hadronization.

All simulated samples were produced using NNPDF3.0 [51] parton distribution functions (PDFs), processed with the full CMS detector model based on GEANT4 [52], and reconstructed with the same suite of programs as used for collision data. Pileup effects are taken into account by superimposing minimum bias events on the hard scattering interac-

JHEP09(2018)148

tion. The simulated samples are reweighted to match the reconstructed vertex multiplicity distribution observed in data.

The particle-flow (PF) event algorithm [53] aims to reconstruct and identify each individual particle in an event, based on an optimized combination of information from the various elements of the CMS detector. The energy of photons is directly obtained from the ECAL measurement, corrected for zero-suppression effects. The energy of electrons is determined from a combination of the electron momentum at the primary interaction vertex as determined by the tracker, the energy of the corresponding ECAL cluster, and the energy sum of all bremsstrahlung photons spatially compatible with originating from the electron track. The energy of muons is obtained from the curvature of the reconstructed muon track. The energy of charged hadrons is determined from a combination of their momentum measured in the tracker and the matching ECAL and HCAL energy deposits, corrected for zero-suppression effects and for the response function of the calorimeters to hadronic showers. Finally, the energy of neutral hadrons is obtained from the corresponding corrected ECAL and HCAL energy deposits.

The events must contain at least one reconstructed primary vertex with at least four associated tracks, with transverse (longitudinal) coordinates required to be within 2 (24) cm of the nominal collision point. The reconstructed vertex with the largest value of summed physics-object p_{T}^2 is taken to be the primary interaction vertex. The physics objects are the jets, clustered using the jet finding algorithm [54, 55] with the tracks assigned to the vertex as inputs, and the associated missing transverse momentum, taken as the negative vector sum of the transverse momenta of those jets.

Electron candidates must pass loose identification criteria based on the shower shape variables, on the ratio of energy deposits in the associated HCAL and ECAL cells, on the geometrical matching between the energy deposits and the associated track, and on the consistency between the energy reconstructed in the calorimeter and the momentum measured in the tracker [42].

Muon candidates are reconstructed from tracks found in the muon system that are associated with the tracks in the inner tracking systems. One muon candidate is required to pass a loose identification [56]. Another muon candidate is required to pass a tighter identification based on the numbers of associated hits found in the pixel and strip trackers, on the numbers of hits and track segments in the muon detector, and on criteria for the matching between the silicon detector track and the muon track segments [56].

Leptons are required to be isolated from other energy deposits in the event. This is expected for signal leptons from Z boson decays, but is not the case for backgrounds from nonprompt leptons originating, e.g., from b hadron decays. The relative isolation of a lepton is defined as the scalar sum of the transverse momenta of all relevant PF candidates within a cone around the lepton, divided by the p_{T} of the lepton candidate. For an electron, the cone size $\Delta R = \sqrt{(\Delta\eta)^2 + (\Delta\phi)^2}$ depends on its p_{T}:

$$\Delta R = \begin{cases} 0.2, & \text{for } p_{\mathrm{T}} \leq 50\,\mathrm{GeV}, \\ \frac{10\,\mathrm{GeV}}{p_{\mathrm{T}}}, & \text{for } 50 < p_{\mathrm{T}} \leq 200\,\mathrm{GeV}, \text{ and} \\ 0.05, & \text{for } p_{\mathrm{T}} > 200\,\mathrm{GeV}. \end{cases} \tag{3.1}$$

JHEP09(2018)148

The electron isolation is based on the photons, and charged and neutral hadrons found in the isolation cone. Charged hadrons originating from pileup vertices are excluded from the sum. The contribution to the isolation sum from neutral pileup particles is accounted for by using the average energy density method [57]. The varying isolation cone radius in eq. (3.1) takes into account the aperture of b hadron decays as a function of their p_{T}, and reduces the inefficiency from accidental overlap of electrons from Z boson decays and jets. For muons, a fixed cone of a size $\Delta R = 0.3$ is used, and the isolation is based on all charged-particle tracks within the isolation cone, excluding the candidate muon track. In the case of two spatially close muons in the event, with overlapping isolation cones, both muons are excluded from each isolation sum. This procedure, together with the use of a variable cone size for electron isolation, ensures high lepton identification efficiency even in the topologies where a Z boson has a high Lorentz boost, as expected for Z bosons produced in a decay of a heavy resonance. The relative isolation of electron and muon candidates is required to be less than 0.1.

Photon identification is based on a multivariate analysis, employing a boosted decision tree algorithm [58, 59]. The inputs to the algorithm include shower shape variables, isolation sums computed from PF candidates in a cone of radius $\Delta R = 0.3$ around the photon candidate, and variables that account for the dependences of the shower shape and isolation variables on the pileup [60]. In addition, a conversion-safe electron veto [60] is applied. Photon candidates are required to pass a working point that corresponds to a typical photon reconstruction and identification efficiency of 90%, in the photon p_{T} range used in the analysis.

In the Jγ channel, large-cone jets are used to reconstruct hadronically decaying highly Lorentz boosted Z boson candidates. Jets are reconstructed from PF candidates clustered using the anti-k_{T} algorithm [54] with a distance parameter of 0.8. Charged hadrons not originating from the primary vertex are not considered in the jet clustering. Corrections based on the jet area [57] are applied to remove the energy contribution of neutral hadrons from pileup interactions. The energies of the jets are further corrected for the response function of the calorimeter. These corrections are extracted from simulation and confirmed with in situ measurements using the energy balance in dijet, multijet, γ+jet, and leptonically decaying Z+jet events [61, 62]. Additional quality criteria are applied to jets to remove rare spurious noise patterns in the calorimeters, and also to suppress leptons misidentified as jets. The jet energy resolution amounts typically to 15% at 10 GeV, 8% at 100 GeV, and 4% at 1 TeV. Jets must have $p_{\mathrm{T}} > 200\,\mathrm{GeV}$ and $|\eta| < 2.0$. The requirement on the jet η suppresses background from γ+jets and QCD multijet events, and ensures that the core of the jet is within the tracker volume of the detector ($|\eta| < 2.5$). The latter requirement is important for subsequent b quark tagging.

Events in the $\ell\ell\gamma$ channel are required to have two same-flavor leptons (electrons or muons) and a photon. Additionally, leptons in the $\mu\mu\gamma$ channel are required to have opposite electric charge. This requirement is not used in the eeγ channel due to a nonnegligible probability to misreconstruct the charge of an electron candidate because of an energetic bremsstrahlung. The leading electron (muon) is required to have $p_{\mathrm{T}} > 65\,(52)\,\mathrm{GeV}$ and $|\eta| < 2.5\,(2.4)$. The subleading lepton is required to have $p_{\mathrm{T}} > 10\,\mathrm{GeV}$ and to be found in

JHEP09(2018)148

the same pseudorapidity range as the leading lepton. The photon in the eeγ ($\mu\mu\gamma$) channel is required to satisfy $p_{\mathrm{T}} > 65\,(40)$ GeV and $|\eta| < 2.5$. Electrons and photons in the ECAL barrel-endcap transition region ($1.44 < |\eta| < 1.57$) are excluded from the analysis. In the eeγ channel, the p_{T} thresholds on the electrons and photons in the ECAL endcap region are increased to 70 GeV, in order to ensure a fully efficient trigger. Photons are required to be separated from lepton candidates by $\Delta R > 0.4$, to reduce the background from final-state radiation in $\mathrm{Z} \to \ell\ell$ events. The invariant mass of the dilepton system is required to be $50 < m_{\ell\ell} < 130$ GeV. The minimum dilepton mass requirement suppresses contributions from $\mathrm{pp} \to \gamma\gamma^{*}$ events, where an internal conversion of a photon produces a lepton pair. Finally, we require the ratio of the photon p_{T} to $m_{\mathrm{Z}\gamma}$ to be greater than 0.27. This requirement suppresses backgrounds due to jets misidentified as photons, without significant loss in the signal efficiency and without introducing a bias in the $m_{\mathrm{Z}\gamma}$ spectrum. We search for resonances in the $m_{\mathrm{Z}\gamma}$ spectrum above 300 (250) GeV in the electron (muon) channel.

For the Jγ channel, the photon candidates are required to have $p_{\mathrm{T}} > 200$ GeV and to fall within the barrel fiducial region of the ECAL ($|\eta| < 1.44$). Events with a photon reconstructed in the endcap region suffer from high γ+jets background and do not add to the sensitivity of the analysis; therefore they are not considered. Photon candidates in the event are required to be separated from large-radius jets by a distance of $\Delta R > 1.1$, which guarantees that the photon isolation cone is not contaminated with the jet constituents.

To identify Z boson candidates in the Jγ channel, the reconstructed large-radius jet mass, evaluated after applying a jet pruning algorithm [63, 64], is used. The jet pruning reclusters the jet constituents and eliminates soft, large-angle QCD radiation, which otherwise contributes significantly to the jet mass. The pruning algorithm reclusters each jet starting from its original constituents with the Cambridge-Aachen (CA) algorithm [65] and discards soft and wide-angle recombinations in each step of the iterative CA procedure. The pruned jet mass ($m_{\mathrm{J}}^{\mathrm{pruned}}$) is computed from the sum of the four-momenta of the remaining constituents, which are corrected with the same factor as has already been used in the generic jet reconstruction described above. A detailed description of the pruning algorithm can be found in ref. [66]. For the signal selection, we require a Z candidate to have $75 < m_{\mathrm{J}}^{\mathrm{pruned}} < 105$ GeV.

Finally, in the Jγ channel a requirement is imposed on the ratio of photon p_{T} to the reconstructed Zγ mass of $p_{\mathrm{T}}/m_{\mathrm{Z}\gamma} > 0.34$, with the cutoff chosen, based on a study of simulated signals and backgrounds, to maximize the discovery potential for a narrow resonance. We search for resonances with masses $m_{\mathrm{Z}\gamma} > 650$ GeV in this channel.

To further discriminate against the QCD multijet and γ+jets backgrounds in the Jγ channel, we categorize the events according to the likelihood of a large-radius jet to contain subjets originating from b quark fragmentation and to contain exactly two subjets. In order to do so, we employ subjet b tagging and N-subjettiness [67] variables (τ_N). The N-subjettiness observable measures the spatial distribution of jet constituents relative to candidate subjet axes in order to quantify how well the jet can be divided into N subjets. Subjet axes are determined by a one-pass optimization procedure, which minimizes N-subjettiness [68]. In particular, the ratio of 2- to 1-subjettiness, $\tau_{21} = \tau_2/\tau_1$, offers an excellent separation between the QCD jets and jets from vector boson decays [69], which tend to have lower τ_{21} values than the former.

JHEP09(2018)148

To infer the presence of b quark subjets within a large-radius jet, pruned jets are split into two subjets by reversing the final iteration of the jet clustering algorithm. These subjets are classified according to the probability of their originating from b quarks, based on results from the combined secondary vertex (CSVv2) b tagging algorithm [70, 71]. A jet is identified as being consistent with the $\mathrm{Z} \to \mathrm{b\bar{b}}$ decay when at least one of its subjets satisfies the medium operating point of the CSVv2 algorithm, and the other subjet satisfies the loose operating point. The medium and loose operating points correspond to 70 and 85% (20 and 50%) in the b jet tagging efficiency for $p_{\mathrm{T}} < 300\,\mathrm{GeV}$ ($p_{\mathrm{T}} = 1\,\mathrm{TeV}$), and 1–2% and 10–15% misidentification probability of a light-flavor jet, respectively. If an event contains a $\mathrm{Z} \to \mathrm{b\bar{b}}$ candidate, it is classified as "b tagged". For the rest of the events, if the large-radius jet has $\tau_{21} < 0.45$, we classify the event as "τ_{21} tagged". Otherwise, the event is assigned to the "untagged" category. These three categories are mutually exclusive and are combined for the final result. The additional classification according to the τ_{21} value enhances signal sensitivity by 10–15% at low to intermediate signal masses (up to ∼2 TeV), relative to a previous analysis in the hadronic channels [32].

4 Background and signal modeling

4.1 Background modeling

Simulations in the $\ell\ell\gamma$ channels indicate that 80–90% of the background remaining after the full event selection is from SM Z boson production accompanied by initial-state photon radiation, with the remainder mostly from Z+jets events, with a jet misreconstructed as a photon. The background $m_{\mathrm{Z}\gamma}$ distributions fall steeply and smoothly with increasing mass, in these channels. Likewise, studies for the Jγ channel based on simulated background samples and on the lower sideband of the jet mass distribution ($50 < m_{\mathrm{J}}^{\mathrm{pruned}} < 70\,\mathrm{GeV}$) in data show that the invariant mass distribution $m_{\mathrm{Z}\gamma}$ of the SM background also falls smoothly in this channel, and that the distributions of kinematic observables derived from the lower jet mass sideband match those for the signal selection.

The background is measured directly in data, through unbinned maximum-likelihood fits to the observed $m_{\mathrm{Z}\gamma}$ distributions, performed separately in each channel. The background in each channel is parametrized with an empirical function. Different families of functions inspired by the ones used in searches for beyond-the-SM phenomena in the dijet, multijet, diphoton, and VV channels at hadron colliders are evaluated in the signal region using simulation ($\ell\ell\gamma$ channels) or the lower jet mass sideband (Jγ channel). Examples of these functions are: $f(x) = P_0(1 - x^{1/3})^{P_1}/x^{P_2+P_3(\ln x)}$ [72], $g(x) = P_0(1 - x)^{P_1}/x^{P_2+P_3(\ln x)}$ [73], $h(x) = P_0 x^{P_1}\exp(P_2 x + P_3 x^2)$ [74], where $x = m_{\mathrm{Z}\gamma}/\sqrt{s}$, $\sqrt{s}$ is the center-of-mass energy (13 TeV), and the number of the fit parameters P_i shown is the maximum order considered. The choice of the order within a family of fitting functions for the background distribution is made independently in each channel using the Fisher F-test [75], which balances the quality of the fit against the number of parameters. The choice among the families of functions is optimized based on the results of the bias test

JHEP09(2018)148

described below. The same function [76] was chosen in both the $\ell\ell\gamma$ and Jγ channels:

$$\frac{\mathrm{d}N}{\mathrm{d}m_{\mathrm{Z}\gamma}} = P_0\, x^{P_1+P_2(\ln x)}, \tag{4.1}$$

where P_0 is a normalization parameter, and P_1, P_2 describe the shape of the invariant mass distribution.

In the $\ell\ell\gamma$ channels, the absence of significant bias in the fit to background is verified by generating a large number of pseudo-experiments using the simulated background shapes, fitting them with different background models, and measuring the difference between the input and fitted background yields in various $m_{\mathrm{Z}\gamma}$ windows within the entire search range. A pull variable is defined in each window by the difference between the input and fitted yields, divided by the combined statistical uncertainties in the data and the fit. If the absolute value of the median in the pull distribution is found to be >0.5, an additional uncertainty is assigned to the background parametrization. A modified pull distribution is then constructed, increasing the statistical uncertainty by an extra term, denoted as the bias term. The bias term is parametrized as a smooth function of $m_{\mathrm{Z}\gamma}$ and tuned to make the absolute value of the median of the modified pull distribution to be <0.5 in all mass windows. This additional uncertainty is included in the likelihood function by adding to the background model a component with a distribution that is the same as the signal, but a normalization coefficient distributed as a Gaussian of mean zero, and a width equal to the integral of the bias term over the signal mass window, defined as the full width at half maximum. The inclusion of this additional component takes into account the possible mismodeling of the background shape. The bias term in the $\ell\ell\gamma$ analysis corresponds to ≈0.3 events/GeV at $m_{\mathrm{Z}\gamma} = 400\,\mathrm{GeV}$ and smoothly falls to $\approx 2 \times 10^{-4}$ events/GeV around $m_{\mathrm{Z}\gamma} = 2\,\mathrm{TeV}$. The observed $m_{\mathrm{Z}\gamma}$ invariant mass spectra in data are shown in figure 1 for the eeγ (left) and $\mu\mu\gamma$ (right) channels. The results of the fits and their uncertainties at 68% confidence level (CL) are shown by the lines and the shaded bands, respectively.

Similarly, in the Jγ channel, the mass spectra in the three analysis categories, derived either from the low jet mass sideband in data or from simulated background samples, are fitted with a variety of alternative functions to generate pseudo-data sets. Additionally, in a set of pseudo-experiments, signals with different mass values and cross sections close to the expected 95% CL limits are injected. The full spectra are fitted with the chosen function of eq. (4.1) together with a signal model (discussed in section 4.2), and the signal cross section is extracted. Distributions of the difference between the data and the fits, divided by the overall uncertainty for the obtained signal cross section, are constructed, and their shapes are found to be consistent with a normal distribution with a mean less than 0.5 and a width consistent with unity.

Thus, any possible systematic bias from the choice of the functional form in the region of low background is proven to be small compared to the statistical uncertainty from the accuracy of the measurements. In the region of large background, the uncertainty in the signal efficiency (discussed in section 5) completely dominates the effect of the background uncertainty on the limits. Thus we assign the statistical uncertainty in the fits as the only uncertainty in the background predictions. The observed $m_{\mathrm{Z}\gamma}$ invariant mass spectra in

JHEP09(2018)148

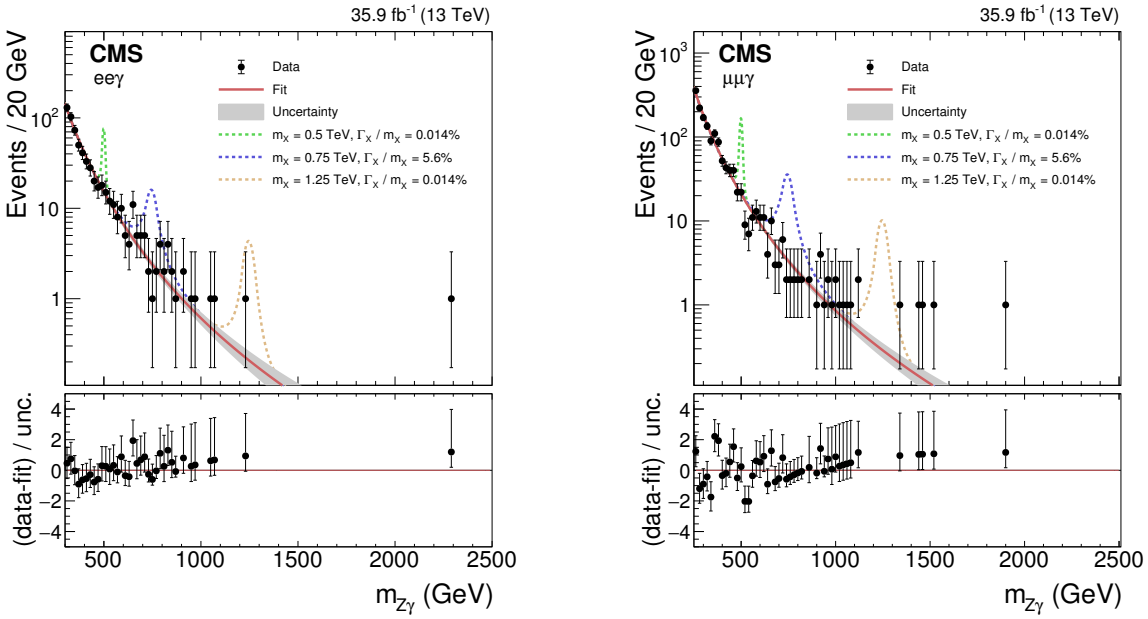

Figure 1. Observed $m_{Z\gamma}$ invariant mass spectra in the eeγ (left) and $\mu\mu\gamma$ (right) channels. The best fits to the background-only hypotheses are represented by the red lines, with their 68% CL uncertainty bands given by the gray shadings. Several narrow and broad signal benchmarks with arbitrary normalization are shown on top of the background prediction with the dashed lines. The lower panels show the difference between the data and the fits, divided by the uncertainty, which includes the statistical uncertainties in the data and the fit. For bins with a small number of entries, the error bars correspond to the Garwood confidence intervals [77].

the signal region ($75 < m_{\mathrm{J}}^{\mathrm{pruned}} < 105\,\mathrm{GeV}$) for the b-tagged, τ_{21}-tagged, and untagged categories, along with the corresponding fits, are shown in figure 2.

4.2 Signal modeling

The signal distribution in $m_{Z\gamma}$ is obtained from the generated events that pass the full selection. The signal shape is parametrized with a Gaussian core and two power-law tails, namely an extended form of the Crystal Ball (CB) function [78]. We find this functional form to provide an adequate description for both narrow and broad signals in the entire mass range used in the analysis. To derive the signal shapes for the intermediate mass values where simulation points are not available, a linear morphing [79] of the shapes obtained from the simulation is used. The typical mass resolution for narrow-width signal events is 1% for the eeγ channel, 1–2% for the $\mu\mu\gamma$ channel, depending on the mass of the resonance, and 3% in the Jγ channel.

The product of signal acceptance and efficiency for a narrow resonance in the eeγ ($\mu\mu\gamma$) channel rises from about 27 (42)% at $m_{Z\gamma} = 0.35\,\mathrm{TeV}$ to about 46 (55)% at $m_{Z\gamma} = 2\,\mathrm{TeV}$, and remains steady until 4 TeV. In the Jγ channel, the product of signal acceptance and efficiency for narrow resonances increases from 7 (3)% at 0.65 TeV to 9 (9)% at 4 TeV in the untagged (τ_{21}-tagged) category, and is between 2 and 3% for the b-tagged category for the resonance masses between 0.65 and 4 TeV.

JHEP09(2018)148

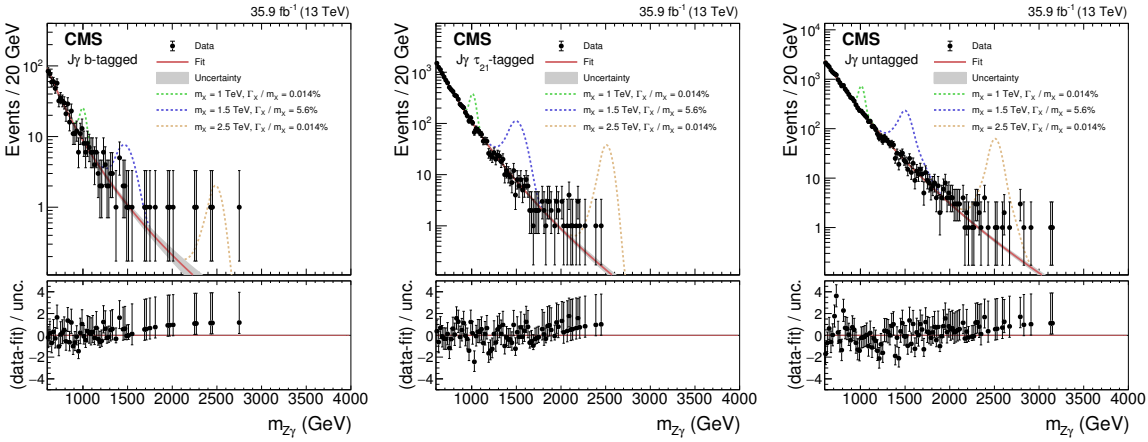

Figure 2. Observed $m_{Z\gamma}$ invariant mass spectra in the Jγ channel in the b-tagged (left), τ_{21}-tagged (center), and untagged (right) categories. The best fits to the background-only hypotheses are represented by the red lines, with their 68% CL uncertainty bands given by the gray shadings. Several narrow and broad signal benchmarks with arbitrary normalization are shown on top of the background prediction with the dashed lines. The lower panels show the difference between the data and the fits, divided by the uncertainty, which includes the statistical uncertainties in the data and the fit. For bins with a small number of entries, the error bars correspond to the Garwood confidence intervals [77].

For a broad resonance the product of signal acceptance and efficiency is similar to the narrow-resonance case up to 2 TeV. At large resonance masses (>2 TeV), however, the effect of rapidly falling PDFs introduces a lower tail in the signal mass distribution. The exact characteristics of this tail are quite sensitive to the resonant line shape. We therefore truncate the mass distribution of the resonance to correspond to the core of the line shape, defined as a window centered on the maximum of the CB function with a width given by ± 5 times the CB function parameter σ, describing the standard deviation of its Gaussian core. The tails outside this window are conservatively discarded in the signal acceptance calculations and when fitting the data. As a result, the product of signal acceptance and efficiency falls to 2% at 4 TeV for the eeγ and $\mu\mu\gamma$ events, to 0.2% in the untagged and τ_{21}-tagged categories, and to <0.1% in the b-tagged category.

5 Systematic uncertainties

The statistical uncertainty in the fits of the background function to data is taken for the background uncertainty in all channels.

The following systematic uncertainties in the signal are defined below, and summarized in table 1:

- Integrated luminosity: the uncertainty in the CMS integrated luminosity is based on cluster counting in the silicon pixel detector and amounts to 2.5% [80].
- PDFs: a 1.0–3.5% uncertainty in the signal efficiency that takes into account the variation in the kinematic acceptance of the analysis is estimated using replicas of

JHEP09(2018)148

the NNPDF3.0 set, following the PDF4LHC prescription [81]. The uncertainty in the signal cross section due to the PDF choice is not considered.

- Pileup: the uncertainty due to the pileup description in the signal simulation, evaluated by changing the total inelastic cross section governing the average multiplicity of pileup interactions by ±5.0% [82], translates to a 1.0% uncertainty in the signal acceptance in all channels.

- Trigger: the uncertainty due to the trigger efficiency differences in data and simulation in the $\ell\ell\gamma$ analysis is estimated with dedicated studies with leptons from Z boson decays and amounts to 1.0 (3.5)% for the eeγ ($\mu\mu\gamma$) channel. In the Jγ channel, a 2.0% uncertainty covers the variation of the trigger efficiency across the mass range probed in the analysis.

- Photon efficiency: the systematic uncertainty due to the differences in the photon identification efficiency between data and simulation is evaluated with $\mathrm{Z} \to \mathrm{ee}$ events in which the electrons are used as proxies for photons, and amounts to 1.5% [60].

- Lepton efficiency: the systematic uncertainty due to the differences in the lepton identification efficiency in data and simulation is evaluated with $\mathrm{Z} \to \mathrm{ee}$ ($\mu\mu$) events and amounts to 2.5 (2.0)% in the eeγ ($\mu\mu\gamma$) channel.

- b tagging efficiency: the uncertainty due to the difference in the b tagging efficiency in data and simulation is estimated from control samples in data and simulation enriched in b quarks [71], and translates into a 15–32% uncertainty in the signal yield in the Jγ channel. It is anticorrelated between the b-tagged and the other two categories, as it induces signal migration between the categories.

- τ_{21} tagging efficiency: to account for the difference between the τ_{21} distributions in data and simulation, a scale factor of 0.97 ± 0.06 [69] is introduced for simulated signal samples. This translates into an uncertainty of 10–12% in the signal yield in the τ_{21}-tagged category and is anticorrelated with that in the untagged category.

- Electron and photon energy scale and resolution: the electron and photon energy scale is known with 0.1–5.0% precision, depending on the energy. This uncertainty is based on the accuracy of the energy scale at the Z boson peak and its extrapolation to higher masses, and translates into a 0.2–4.6 (0.1–2.3)% correlated uncertainty in the $m_{\mathrm{Z}\gamma}$ scale in the eeγ channel ($\mu\mu\gamma$ and Jγ channels). The uncertainty in the electron and photon energy resolution based on the Gaussian smearing evaluated at the Z boson peak translates to a 10 (5)% uncertainty in the $m_{\mathrm{Z}\gamma}$ resolution in the eeγ channel ($\mu\mu\gamma$ and Jγ channels).

- Muon momentum scale and resolution: the muon momentum scale is measured with 0.1–5.0% precision up to $p_{\mathrm{T}} = 200\,\mathrm{GeV}$, with an additional 0.1–6.0% uncertainty at higher values, resulting in a 0.1–4.6% uncertainty in the $m_{\mathrm{Z}\gamma}$ mass scale in the $\mu\mu\gamma$ channel. A 10% uncertainty in the $m_{\mathrm{Z}\gamma}$ resolution in the $\mu\mu\gamma$ channel is conservatively assigned to account for the uncertainty in the muon momentum resolution.

JHEP09(2018)148

Source	eeγ	$\mu\mu\gamma$	b-tagged	τ_{21}-tagged	Untagged
Integrated luminosity	2.5%	2.5%	2.5%	2.5%	2.5%
PDFs	1–3.5%	1–3.5%	1–3.5%	1–3.5%	1–3.5%
Pileup	1%	1%	1%	1%	1%
Trigger	1%	3.5%	2%	2%	2%
Photon efficiency	1.5%	1.5%	1.5%	1.5%	1.5%
Lepton efficiency	2.5%	2%	—	—	—
b tagging efficiency	—	—	15–32%	anticorr.	anticorr.
τ_{21} tagging efficiency	—	—	—	10–12%	anticorr.
e/γ energy scale	0.2–4.6%	0.1–2.3%	0.1–2.3%	0.1–2.3%	0.1–2.3%
e/γ energy resolution	10%	5%	5%	5%	5%
Muon momentum scale	—	0.1–4.6%	—	—	—
Muon momentum resolution	—	10%	—	—	—
JES and JER	—	—	3.2%	3.2%	3.2%
JMS and JMR	—	—	4.1%	4.1%	4.1%

Table 1. Summary of the systematic uncertainties in the signal yield (upper part of the table) or shape (lower part of the table). A dash indicates that the uncertainty does not apply.

- Jet energy scale (JES), jet mass scale (JMS), jet energy resolution (JER), and jet mass resolution (JMR): the uncertainties [61, 62, 66] are propagated to all the relevant quantities, and affect both the signal yield and its shape. The overall effect of these uncertainties added in quadrature corresponds to approximately 5.0% uncertainty in the signal yield, as determined by changing the four-momenta of the jets accordingly and carrying out the full analysis with the modified quantities.

6 Results

The data are consistent with the background-only expectations in all channels. We set upper limits on the production cross section of heavy spin-0 resonances using the asymptotic approximation [83] of the modified frequentist CL_s method [84–86], with a likelihood ratio used as a test statistic, and uncertainties incorporated as nuisance parameters with log-normal (normalization) or Gaussian (shape) priors. The limits are set in the mass range between 0.35 (0.30) and 4.0 TeV in the eeγ ($\mu\mu\gamma$) channel and 0.65–4.0 TeV in the Jγ channel. We note that the asymptotic approximation tends to produce lower cross section limits than the exact CL_s calculations in the regions with low background. We tested that the difference is at most 4 (30)% for resonance masses below 1 TeV (around 3 TeV).

JHEP09(2018)148

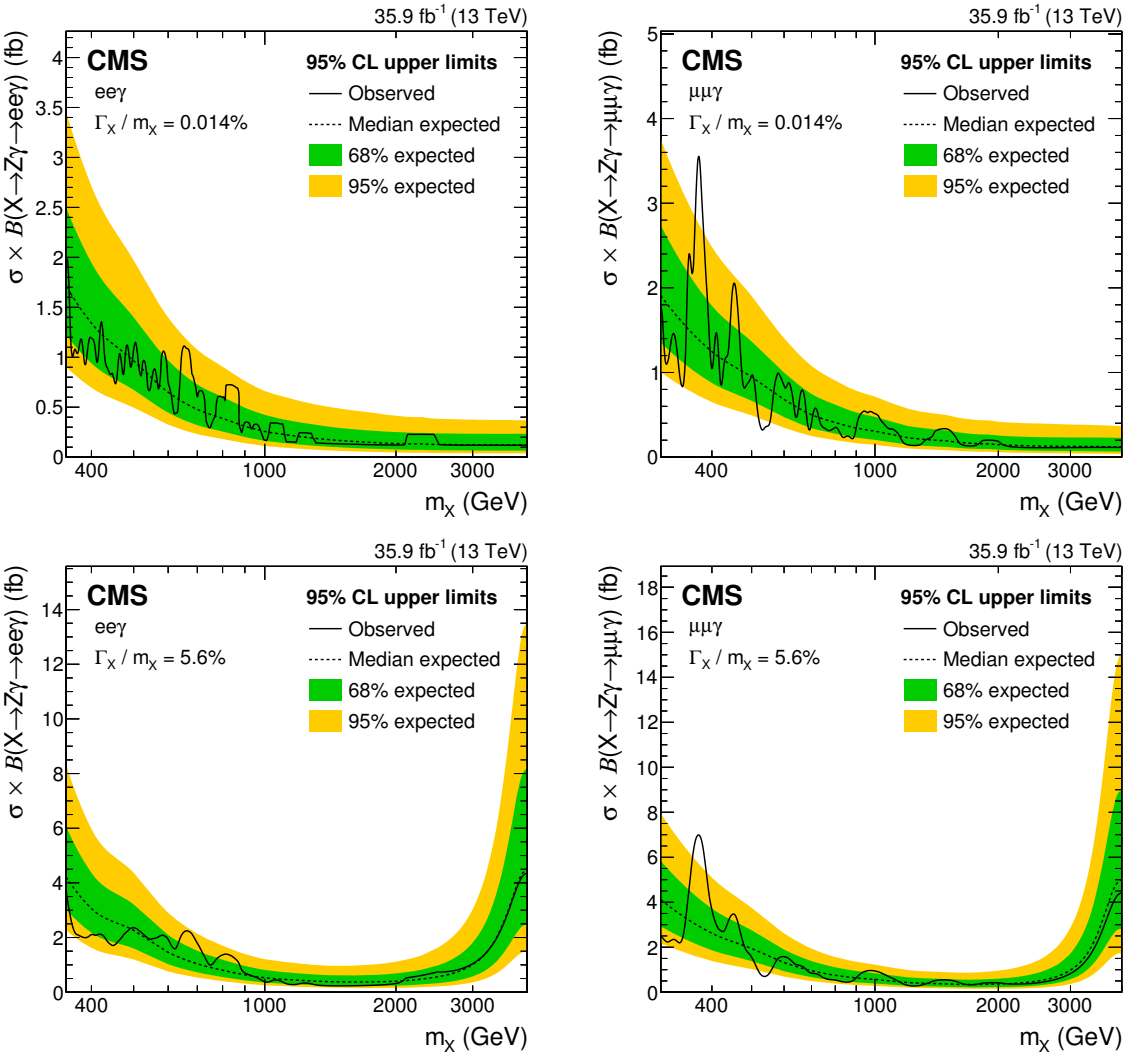

Figure 3. Observed (solid) and expected (dashed) 95% CL upper limits on $\sigma(\mathrm{X} \to \mathrm{Z}\gamma)\,\mathcal{B}(\mathrm{Z} \to \ell\ell\gamma)$, as a function of signal mass m_{X} for the eeγ (left column) and $\mu\mu\gamma$ (right column) channels, and for narrow (upper row) and broad (lower row) spin-0 resonances. The green and yellow shaded bands correspond to respective 68 and 95% CL ranges in the expected limits for the background-only hypothesis.

6.1 The $\ell\ell\gamma$ channels

Figure 3 shows the observed and expected 95% CL upper limits on the product of signal cross section and branching fraction to the $\ell\ell\gamma$ final state, $\sigma(\mathrm{X} \to \mathrm{Z}\gamma)\,\mathcal{B}(\mathrm{Z} \to \ell\ell\gamma)$, as a function of the resonance mass, for the eeγ channel (left column) and the $\mu\mu\gamma$ channel (right column), for narrow (upper row) and broad (lower row) resonances. The expected limits for the background-only hypothesis are represented by the dashed black lines, and their 68 and 95% CL ranges are shown with the green and yellow bands, respectively. The observed limits are represented by the solid black lines. The highest observed deviation is found in the $\mu\mu\gamma$ channel at the mass of approximately 350 GeV and corresponds to a local (global)

JHEP09(2018)148

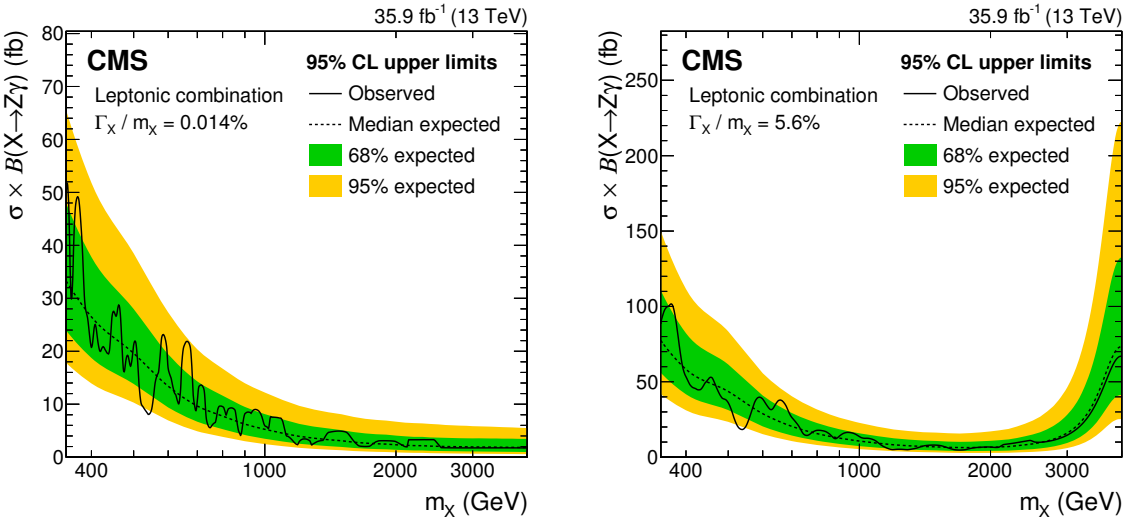

Figure 4. Observed (solid) and expected (dashed) 95% CL upper limits on $\sigma(\mathrm{X} \to \mathrm{Z}\gamma)$ as a function of signal mass m_{X}, together with the 68% (green) and 95% (yellow) CL ranges of the expected limit for the background-only hypothesis, for the combination of the eeγ and $\mu\mu\gamma$ channels for (left) narrow and (right) broad spin-0 resonances.

significance of approximately 3.0 (2.1) standard deviations for a narrow resonance. The limits on $\sigma(\mathrm{X} \to \mathrm{Z}\gamma)$, obtained by combining the two leptonic search channels and taking into account the leptonic branching fraction of the Z boson decays [87], are shown in figure 4. The rapid increase in the limit for a broad resonance with a mass above approximately 3 TeV is due to a significant low-mass tail in the resonance line-shape extending outside the truncation window, as discussed in section 4.2.

6.2 The Jγ channel

The observed and expected 95% CL upper limits on the product of signal cross section and branching fraction in the Zγ channel, $\sigma(\mathrm{X} \to \mathrm{Z}\gamma)$ for narrow and broad resonances in the b-tagged, τ_{21}-tagged, and untagged categories are presented in figure 5. The results based on the combination of the three categories for both narrow and broad resonances are shown in figure 6. The combination includes the (anti)correlation of systematic uncertainties between the three categories. We observe a small deviation at a mass $\approx$2 TeV with local significance of 2.7 (3.6) standard deviations for the narrow (broad) resonance width hypothesis. The global significance of this excess is 1.8 (2.8) standard deviations.

6.3 Combination of the $\ell\ell\gamma$ and Jγ channels

The results based on the combination of the $\ell\ell\gamma$ and Jγ channels are shown in figure 7, assuming uncorrelated uncertainties between the leptonic and hadronic channels, except for the uncertainties in the integrated luminosity, PDFs, and photon energy scale, which are taken as fully correlated among all the channels. These are the most stringent limits on resonances decaying in the Zγ channel to date in the mass range probed.

JHEP09(2018)148

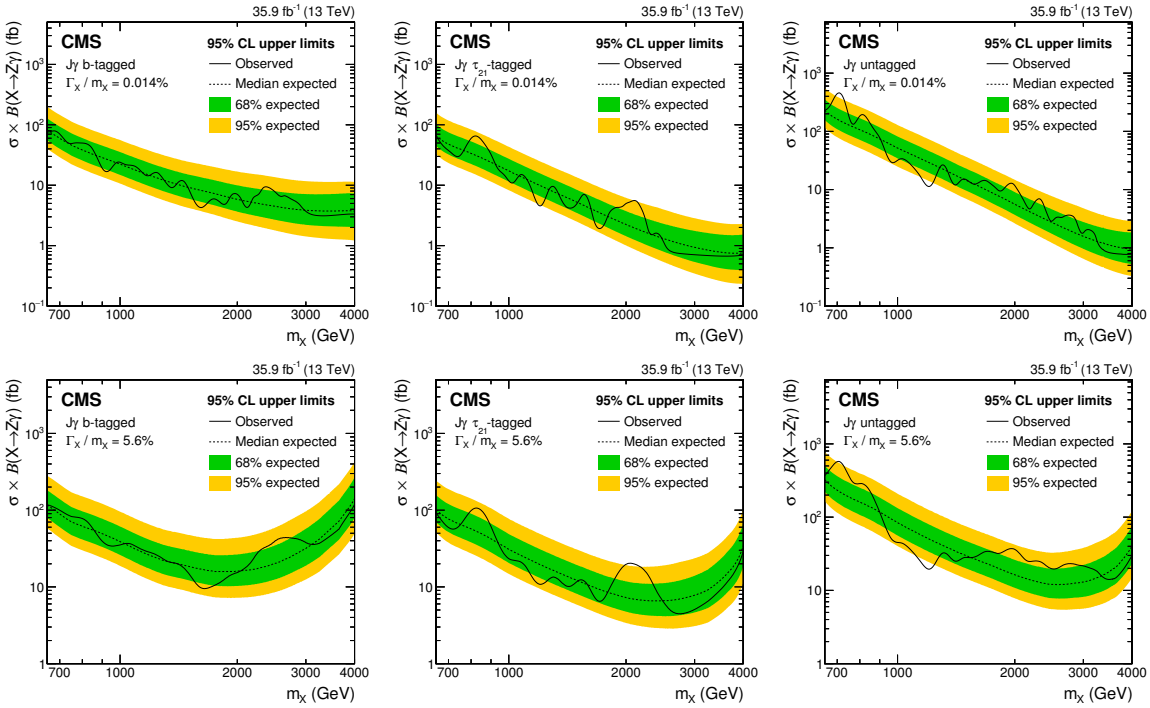

Figure 5. Observed (solid) and expected (dashed) 95% CL upper limits on $\sigma(\mathrm{X} \to \mathrm{Z}\gamma)$, as a function of signal mass m_{X}, for the b-tagged (left column), τ_{21}-tagged (middle column), and untagged (right column) categories, and for narrow (upper row) and broad (lower row) spin-0 resonances. The colored bands correspond to the 68% (green) and 95% (yellow) CL ranges of the expected limit for the background-only hypothesis.

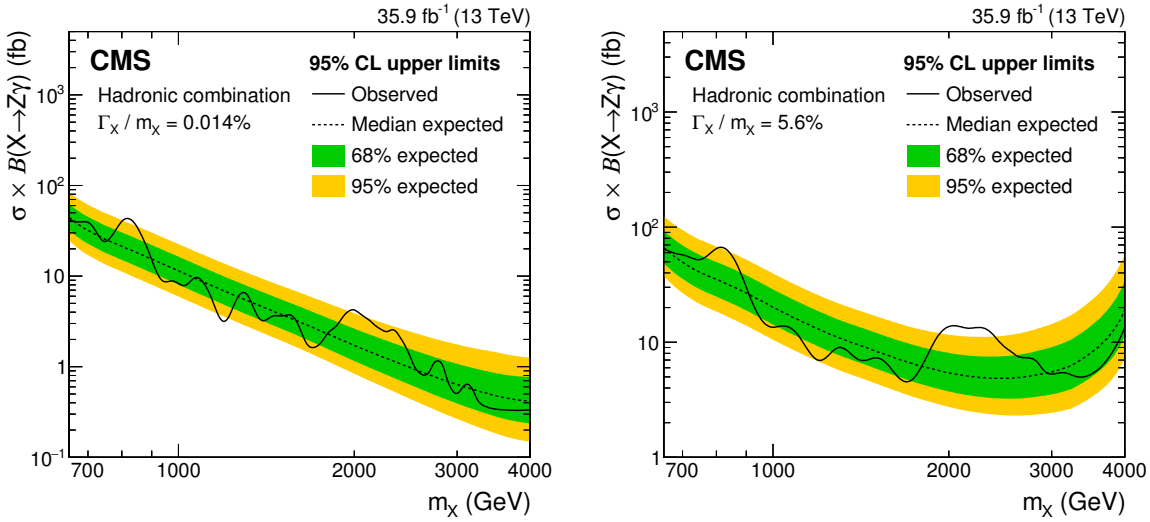

Figure 6. Observed (solid) and expected (dashed) 95% CL upper limits on $\sigma(\mathrm{X} \to \mathrm{Z}\gamma)$ as a function of signal mass m_{X}, together with the 68% (green) and 95% (yellow) CL ranges of the expected limit for the background-only hypothesis, for the combination of the b-tagged, τ_{21}-tagged, and untagged categories for (left) narrow and (right) broad spin-0 resonances.

JHEP09(2018)148

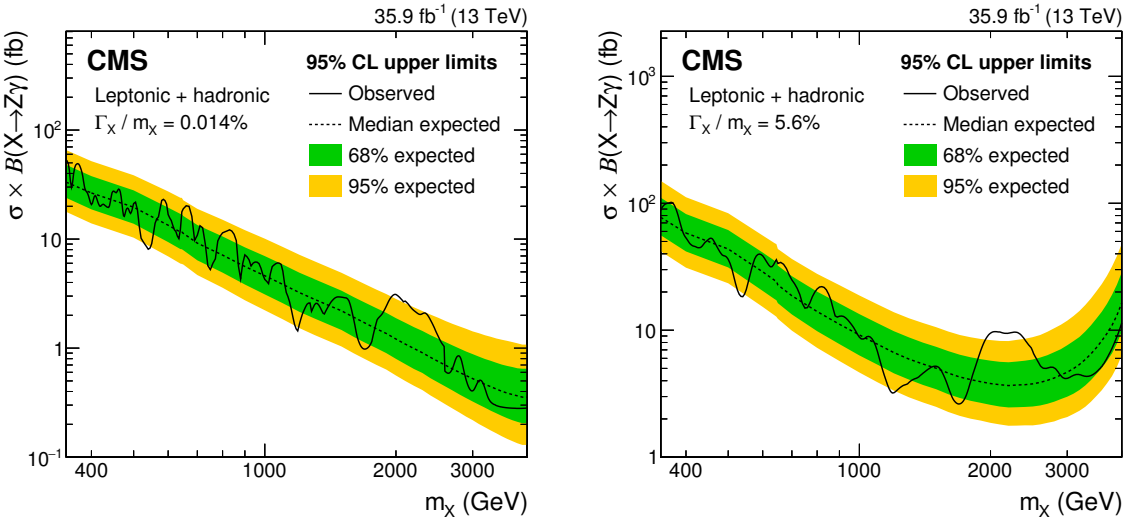

Figure 7. Observed and expected limits on the product of the production cross section and branching fraction $\mathcal{B}(\mathrm{X} \to \mathrm{Z}\gamma)$, as a function of signal mass m_{X}, for (left) narrow and (right) broad spin-0 resonances, obtained from the combination of the leptonic and hadronic decay channels.

7 Summary

A search is presented for resonances decaying to a Z boson and a photon. The analysis is based on data from proton-proton collisions at a center-of-mass energy of 13 TeV, corresponding to an integrated luminosity of 35.9 fb^{-1}, collected with the CMS detector at the LHC in 2016. Two decay modes of the Z boson are investigated. In the leptonic channels, the Z boson candidates are reconstructed using electron or muon pairs. In the hadronic channels, they are identified using a large-radius jet, containing either light-quark or b quark decay products of the Z boson, via jet substructure and advanced b tagging techniques. The results from these channels are combined and interpreted in terms of upper limits on the product of the production cross section and the branching fraction to $\mathrm{Z}\gamma$ for narrow (broad) spin-0 resonances with masses between 0.35 and 4.0 TeV, ranging from 50 (100) to 0.3 (1.5) fb. These are the most stringent limits on such resonances to date.

Acknowledgments

We congratulate our colleagues in the CERN accelerator departments for the excellent performance of the LHC and thank the technical and administrative staffs at CERN and at other CMS institutes for their contributions to the success of the CMS effort. In addition, we gratefully acknowledge the computing centers and personnel of the Worldwide LHC Computing Grid for delivering so effectively the computing infrastructure essential to our analyses. Finally, we acknowledge the enduring support for the construction and operation of the LHC and the CMS detector provided by the following funding agencies: BMWFW and FWF (Austria); FNRS and FWO (Belgium); CNPq, CAPES, FAPERJ, and FAPESP (Brazil); MES (Bulgaria); CERN; CAS, MoST, and NSFC (China); COL-

JHEP09(2018)148

CIENCIAS (Colombia); MSES and CSF (Croatia); RPF (Cyprus); SENESCYT (Ecuador); MoER, ERC IUT, and ERDF (Estonia); Academy of Finland, MEC, and HIP (Finland); CEA and CNRS/IN2P3 (France); BMBF, DFG, and HGF (Germany); GSRT (Greece); OTKA and NIH (Hungary); DAE and DST (India); IPM (Iran); SFI (Ireland); INFN (Italy); MSIP and NRF (Republic of Korea); LAS (Lithuania); MOE and UM (Malaysia); BUAP, CINVESTAV, CONACYT, LNS, SEP, and UASLP-FAI (Mexico); MBIE (New Zealand); PAEC (Pakistan); MSHE and NSC (Poland); FCT (Portugal); JINR (Dubna); MON, RosAtom, RAS, RFBR and RAEP (Russia); MESTD (Serbia); SEIDI, CPAN, PCTI and FEDER (Spain); Swiss Funding Agencies (Switzerland); MST (Taipei); ThEPCenter, IPST, STAR, and NSTDA (Thailand); TUBITAK and TAEK (Turkey); NASU and SFFR (Ukraine); STFC (United Kingdom); DOE and NSF (U.S.A.).

Individuals have received support from the Marie-Curie program and the European Research Council and Horizon 2020 Grant, contract No. 675440 (European Union); the Leventis Foundation; the A. P. Sloan Foundation; the Alexander von Humboldt Foundation; the Belgian Federal Science Policy Office; the Fonds pour la Formation à la Recherche dans l'Industrie et dans l'Agriculture (FRIA-Belgium); the Agentschap voor Innovatie door Wetenschap en Technologie (IWT-Belgium); the Ministry of Education, Youth and Sports (MEYS) of the Czech Republic; the Council of Science and Industrial Research, India; the HOMING PLUS program of the Foundation for Polish Science, cofinanced from European Union, Regional Development Fund, the Mobility Plus program of the Ministry of Science and Higher Education, the National Science Center (Poland), contracts Harmonia 2014/14/M/ST2/00428, Opus 2014/13/B/ST2/02543, 2014/15/B/ST2/03998, and 2015/19/B/ST2/02861, Sonata-bis 2012/07/E/ST2/01406; the National Priorities Research Program by Qatar National Research Fund; the Programa Severo Ochoa del Principado de Asturias; the Thalis and Aristeia programs cofinanced by EU-ESF and the Greek NSRF; the Rachadapisek Sompot Fund for Postdoctoral Fellowship, Chulalongkorn University and the Chulalongkorn Academic into Its 2nd Century Project Advancement Project (Thailand); the Welch Foundation, contract C-1845; and the Weston Havens Foundation (U.S.A.).

References

[1] ATLAS collaboration, *Observation of a new particle in the search for the Standard Model Higgs boson with the ATLAS detector at the LHC*, *Phys. Lett.* **B 716** (2012) 1 [arXiv:1207.7214] [INSPIRE].

[2] CMS collaboration, *Observation of a new boson at a mass of* 125 *GeV with the CMS experiment at the LHC*, *Phys. Lett.* **B 716** (2012) 30 [arXiv:1207.7235] [INSPIRE].

[3] CMS collaboration, *Observation of a new boson with mass near* 125 *GeV in pp collisions at* $\sqrt{s} = 7$ *and* 8 *TeV*, *JHEP* **06** (2013) 081 [arXiv:1303.4571] [INSPIRE].

JHEP09(2018)148

[4] CMS collaboration, *Search for massive resonances in dijet systems containing jets tagged as W or Z boson decays in pp collisions at $\sqrt{s} = 8$ TeV*, *JHEP* **08** (2014) 173 [arXiv:1405.1994] [INSPIRE].

[5] CMS collaboration, *Search for massive resonances decaying into pairs of boosted bosons in semi-leptonic final states at $\sqrt{s} = 8$ TeV*, *JHEP* **08** (2014) 174 [arXiv:1405.3447] [INSPIRE].

[6] ATLAS collaboration, *Combination of searches for WW, WZ and ZZ resonances in pp collisions at $\sqrt{s} = 8$ TeV with the ATLAS detector*, *Phys. Lett.* **B 755** (2016) 285 [arXiv:1512.05099] [INSPIRE].

[7] ATLAS collaboration, *Searches for heavy diboson resonances in pp collisions at $\sqrt{s} = 13$ TeV with the ATLAS detector*, *JHEP* **09** (2016) 173 [arXiv:1606.04833] [INSPIRE].

[8] CMS collaboration, *Search for massive resonances decaying into WW, WZ or ZZ bosons in proton-proton collisions at $\sqrt{s} = 13$ TeV*, *JHEP* **03** (2017) 162 [arXiv:1612.09159] [INSPIRE].

[9] CMS collaboration, *Search for charged Higgs bosons produced via vector boson fusion and decaying into a pair of W and Z bosons using pp collisions at $\sqrt{s} = 13$ TeV*, *Phys. Rev. Lett.* **119** (2017) 141802 [arXiv:1705.02942] [INSPIRE].

[10] CMS collaboration, *Combination of searches for heavy resonances decaying to WW, WZ, ZZ, WH and ZH boson pairs in proton-proton collisions at $\sqrt{s} = 8$ and 13 TeV*, *Phys. Lett.* **B 774** (2017) 533 [arXiv:1705.09171] [INSPIRE].

[11] ATLAS collaboration, *Search for diboson resonances with boson-tagged jets in pp collisions at $\sqrt{s} = 13$ TeV with the ATLAS detector*, *Phys. Lett.* **B 777** (2018) 91 [arXiv:1708.04445] [INSPIRE].

[12] ATLAS collaboration, *Searches for heavy ZZ and ZW resonances in the $\ell\ell qq$ and $\nu\nu qq$ final states in pp collisions at $\sqrt{s} = 13$ TeV with the ATLAS detector*, *JHEP* **03** (2018) 009 [arXiv:1708.09638] [INSPIRE].

[13] ATLAS collaboration, *Search for WW/WZ resonance production in $\ell\nu qq$ final states in pp collisions at $\sqrt{s} = 13$ TeV with the ATLAS detector*, *JHEP* **03** (2018) 042 [arXiv:1710.07235] [INSPIRE].

[14] ATLAS collaboration, *Search for heavy resonances decaying into WW in the $e\nu\mu\nu$ final state in pp collisions at $\sqrt{s} = 13$ TeV with the ATLAS detector*, *Eur. Phys. J.* **C 78** (2018) 24 [arXiv:1710.01123] [INSPIRE].

[15] CMS collaboration, *Search for ZZ resonances in the $2\ell 2\nu$ final state in proton-proton collisions at 13 TeV*, *JHEP* **03** (2018) 003 [arXiv:1711.04370] [INSPIRE].

[16] CMS collaboration, *Search for a massive resonance decaying into a Higgs boson and a W or Z boson in hadronic final states in proton-proton collisions at $\sqrt{s} = 8$ TeV*, *JHEP* **02** (2016) 145 [arXiv:1506.01443] [INSPIRE].

[17] CMS collaboration, *Search for massive WH resonances decaying into the $\ell\nu b\bar{b}$ final state at $\sqrt{s} = 8$ TeV*, *Eur. Phys. J.* **C 76** (2016) 237 [arXiv:1601.06431] [INSPIRE].

[18] ATLAS collaboration, *Search for new resonances decaying to a W or Z boson and a Higgs boson in the $\ell^+\ell^- b\bar{b}$, $\ell\nu b\bar{b}$ and $\nu\bar{\nu}b\bar{b}$ channels with pp collisions at $\sqrt{s} = 13$ TeV with the ATLAS detector*, *Phys. Lett.* **B 765** (2017) 32 [arXiv:1607.05621] [INSPIRE].

JHEP09(2018)148

[19] CMS collaboration, *Search for heavy resonances decaying into a vector boson and a Higgs boson in final states with charged leptons, neutrinos and b quarks*, *Phys. Lett.* **B 768** (2017) 137 [arXiv:1610.08066] [INSPIRE].

[20] CMS collaboration, *Search for heavy resonances that decay into a vector boson and a Higgs boson in hadronic final states at* $\sqrt{s} = 13$ *TeV*, *Eur. Phys. J.* **C 77** (2017) 636 [arXiv:1707.01303] [INSPIRE].

[21] ATLAS collaboration, *Search for heavy resonances decaying to a W or Z boson and a Higgs boson in the* $q\bar{q}^{(\prime)}b\bar{b}$ *final state in pp collisions at* $\sqrt{s} = 13$ *TeV with the ATLAS detector*, *Phys. Lett.* **B 774** (2017) 494 [arXiv:1707.06958] [INSPIRE].

[22] L.D. Landau, *On the angular momentum of a system of two photons*, *Dokl. Akad. Nauk Ser. Fiz.* **60** (1948) 207 [INSPIRE].

[23] C.-N. Yang, *Selection rules for the dematerialization of a particle into two photons*, *Phys. Rev.* **77** (1950) 242 [INSPIRE].

[24] E. Eichten and K. Lane, *Low-scale technicolor at the Tevatron and LHC*, *Phys. Lett.* **B 669** (2008) 235 [arXiv:0706.2339] [INSPIRE].

[25] A. Freitas and P. Schwaller, *Multi-photon signals from composite models at LHC*, *JHEP* **01** (2011) 022 [arXiv:1010.2528] [INSPIRE].

[26] R. Barbieri and R. Torre, *Signals of single particle production at the earliest LHC*, *Phys. Lett.* **B 695** (2011) 259 [arXiv:1008.5302] [INSPIRE].

[27] I. Low, J. Lykken and G. Shaughnessy, *Singlet scalars as Higgs imposters at the Large Hadron Collider*, *Phys. Rev.* **D 84** (2011) 035027 [arXiv:1105.4587] [INSPIRE].

[28] H. Davoudiasl, J.L. Hewett and T.G. Rizzo, *Experimental probes of localized gravity: on and off the wall*, *Phys. Rev.* **D 63** (2001) 075004 [hep-ph/0006041] [INSPIRE].

[29] B.C. Allanach, J.P. Skittrall and K. Sridhar, *Z boson decay to photon plus Kaluza-Klein graviton in large extra dimensions*, *JHEP* **11** (2007) 089 [arXiv:0705.1953] [INSPIRE].

[30] ATLAS collaboration, *Searches for the* $Z\gamma$ *decay mode of the Higgs boson and for new high-mass resonances in pp collisions at* $\sqrt{s} = 13$ *TeV with the ATLAS detector*, *JHEP* **10** (2017) 112 [arXiv:1708.00212] [INSPIRE].

[31] ATLAS collaboration, *Search for heavy resonances decaying to a Z boson and a photon in pp collisions at* $\sqrt{s} = 13$ *TeV with the ATLAS detector*, *Phys. Lett.* **B 764** (2017) 11 [arXiv:1607.06363] [INSPIRE].

[32] CMS collaboration, *Search for high-mass* $Z\gamma$ *resonances in proton-proton collisions at* $\sqrt{s} = 8$ *and* 13 *TeV using jet substructure techniques*, *Phys. Lett.* **B 772** (2017) 363 [arXiv:1612.09516] [INSPIRE].

[33] L3 collaboration, P. Achard et al., *Search for anomalous couplings in the Higgs sector at LEP*, *Phys. Lett.* **B 589** (2004) 89 [hep-ex/0403037] [INSPIRE].

[34] D0 collaboration, V.M. Abazov et al., *Search for particles decaying into a Z boson and a photon in* $p\bar{p}$ *collisions at* $\sqrt{s} = 1.96$ *TeV*, *Phys. Lett.* **B 641** (2006) 415 [*Erratum ibid.* **B 670** (2009) 455] [hep-ex/0605064] [INSPIRE].

[35] D0 collaboration, V.M. Abazov et al., *Search for a scalar or vector particle decaying into* $Z\gamma$ *in* $p\bar{p}$ *collisions at* $\sqrt{s} = 1.96$ *TeV*, *Phys. Lett.* **B 671** (2009) 349 [arXiv:0806.0611] [INSPIRE].

JHEP09(2018)148

[36] ATLAS collaboration, *Measurements of $W\gamma$ and $Z\gamma$ production in pp collisions at $\sqrt{s} = 7$ TeV with the ATLAS detector at the LHC*, *Phys. Rev.* **D 87** (2013) 112003 [*Erratum ibid.* **D 91** (2015) 119901] [arXiv:1302.1283] [INSPIRE].

[37] ATLAS collaboration, *Search for new resonances in $W\gamma$ and $Z\gamma$ final states in pp collisions at $\sqrt{s} = 8$ TeV with the ATLAS detector*, *Phys. Lett.* **B 738** (2014) 428 [arXiv:1407.8150] [INSPIRE].

[38] CMS collaboration, *Search for high-mass $Z\gamma$ resonances in $e^+e^-\gamma$ and $\mu^+\mu^-\gamma$ final states in proton-proton collisions at $\sqrt{s} = 8$ and 13 TeV*, *JHEP* **01** (2017) 076 [arXiv:1610.02960] [INSPIRE].

[39] CMS collaboration, *Search for a Higgs boson decaying into a Z and a photon in pp collisions at $\sqrt{s} = 7$ and 8 TeV*, *Phys. Lett.* **B 726** (2013) 587 [arXiv:1307.5515] [INSPIRE].

[40] ATLAS collaboration, *Search for Higgs boson decays to a photon and a Z boson in pp collisions at $\sqrt{s} = 7$ and 8 TeV with the ATLAS detector*, *Phys. Lett.* **B 732** (2014) 8 [arXiv:1402.3051] [INSPIRE].

[41] CMS collaboration, *Description and performance of track and primary-vertex reconstruction with the CMS tracker*, 2014 *JINST* **9** P10009 [arXiv:1405.6569] [INSPIRE].

[42] CMS collaboration, *Performance of electron reconstruction and selection with the CMS detector in proton-proton collisions at $\sqrt{s} = 8$ TeV*, 2015 *JINST* **10** P06005 [arXiv:1502.02701] [INSPIRE].

[43] CMS collaboration, *Performance of CMS muon reconstruction in pp collision events at $\sqrt{s} = 7$ TeV*, 2012 *JINST* **7** P10002 [arXiv:1206.4071] [INSPIRE].

[44] CMS collaboration, *The CMS trigger system*, 2017 *JINST* **12** P01020 [arXiv:1609.02366] [INSPIRE].

[45] CMS collaboration, *The CMS experiment at the CERN LHC*, 2008 *JINST* **3** S08004 [INSPIRE].

[46] T. Sjöstrand, S. Mrenna and P.Z. Skands, *A brief introduction to PYTHIA* 8.1, *Comput. Phys. Commun.* **178** (2008) 852 [arXiv:0710.3820] [INSPIRE].

[47] P. Skands, S. Carrazza and J. Rojo, *Tuning PYTHIA* 8.1*: the Monash* 2013 *tune*, *Eur. Phys. J.* **C 74** (2014) 3024 [arXiv:1404.5630] [INSPIRE].

[48] CMS collaboration, *Event generator tunes obtained from underlying event and multiparton scattering measurements*, *Eur. Phys. J.* **C 76** (2016) 155 [arXiv:1512.00815] [INSPIRE].

[49] J. Alwall, M. Herquet, F. Maltoni, O. Mattelaer and T. Stelzer, *MadGraph* 5*: going beyond*, *JHEP* **06** (2011) 128 [arXiv:1106.0522] [INSPIRE].

[50] J. Alwall et al., *The automated computation of tree-level and next-to-leading order differential cross sections and their matching to parton shower simulations*, *JHEP* **07** (2014) 079 [arXiv:1405.0301] [INSPIRE].

[51] NNPDF collaboration, R.D. Ball et al., *Parton distributions for the LHC run II*, *JHEP* **04** (2015) 040 [arXiv:1410.8849] [INSPIRE].

[52] GEANT4 collaboration, S. Agostinelli et al., *GEANT4: a simulation toolkit*, *Nucl. Instrum. Meth.* **A 506** (2003) 250 [INSPIRE].

[53] CMS collaboration, *Particle-flow reconstruction and global event description with the CMS detector*, 2017 *JINST* **12** P10003 [arXiv:1706.04965] [INSPIRE].

JHEP09(2018)148

[54] M. Cacciari, G.P. Salam and G. Soyez, *The anti-k_t jet clustering algorithm*, *JHEP* **04** (2008) 063 [arXiv:0802.1189] [INSPIRE].

[55] M. Cacciari, G.P. Salam and G. Soyez, *FastJet user manual*, *Eur. Phys. J.* **C 72** (2012) 1896 [arXiv:1111.6097] [INSPIRE].

[56] CMS collaboration, *Performance of the CMS muon detector and muon reconstruction with proton-proton collisions at $\sqrt{s} = 13$ TeV*, 2018 *JINST* **13** P06015 [arXiv:1804.04528] [INSPIRE].

[57] M. Cacciari and G.P. Salam, *Pileup subtraction using jet areas*, *Phys. Lett.* **B 659** (2008) 119 [arXiv:0707.1378] [INSPIRE].

[58] H.-J. Yang, B.P. Roe and J. Zhu, *Studies of boosted decision trees for MiniBooNE particle identification*, *Nucl. Instrum. Meth.* **A 555** (2005) 370 [physics/0508045] [INSPIRE].

[59] A. Höcker et al., *TMVA — toolkit for multivariate data analysis*, PoS(ACAT)040 [physics/0703039] [INSPIRE].

[60] CMS collaboration, *Performance of photon reconstruction and identification with the CMS detector in proton-proton collisions at $\sqrt{s} = 8$ TeV*, 2015 *JINST* **10** P08010 [arXiv:1502.02702] [INSPIRE].

[61] CMS collaboration, *Determination of jet energy calibration and transverse momentum resolution in CMS*, 2011 *JINST* **6** P11002 [arXiv:1107.4277] [INSPIRE].

[62] CMS collaboration, *Jet energy scale and resolution in the CMS experiment in pp collisions at 8 TeV*, 2017 *JINST* **12** P02014 [arXiv:1607.03663] [INSPIRE].

[63] S.D. Ellis, C.K. Vermilion and J.R. Walsh, *Techniques for improved heavy particle searches with jet substructure*, *Phys. Rev.* **D 80** (2009) 051501 [arXiv:0903.5081] [INSPIRE].

[64] S.D. Ellis, C.K. Vermilion and J.R. Walsh, *Recombination algorithms and jet substructure: pruning as a tool for heavy particle searches*, *Phys. Rev.* **D 81** (2010) 094023 [arXiv:0912.0033] [INSPIRE].

[65] Y.L. Dokshitzer, G.D. Leder, S. Moretti and B.R. Webber, *Better jet clustering algorithms*, *JHEP* **08** (1997) 001 [hep-ph/9707323] [INSPIRE].

[66] CMS collaboration, *Identification techniques for highly boosted W bosons that decay into hadrons*, *JHEP* **12** (2014) 017 [arXiv:1410.4227] [INSPIRE].

[67] J. Thaler and K. Van Tilburg, *Identifying boosted objects with N-subjettiness*, *JHEP* **03** (2011) 015 [arXiv:1011.2268] [INSPIRE].

[68] J. Thaler and K. Van Tilburg, *Maximizing boosted top identification by minimizing N-subjettiness*, *JHEP* **02** (2012) 093 [arXiv:1108.2701] [INSPIRE].

[69] CMS collaboration, *Jet algorithms performance in 13 TeV data*, CMS-PAS-JME-16-003, CERN, Geneva, Switzerland, (2017).

[70] CMS collaboration, *Identification of b-quark jets with the CMS experiment*, 2013 *JINST* **8** P04013 [arXiv:1211.4462] [INSPIRE].

[71] CMS collaboration, *Identification of heavy-flavour jets with the CMS detector in pp collisions at 13 TeV*, 2018 *JINST* **13** P05011 [arXiv:1712.07158] [INSPIRE].

[72] ATLAS collaboration, *Search for strong gravity in multijet final states produced in pp collisions at $\sqrt{s} = 13$ TeV using the ATLAS detector at the LHC*, *JHEP* **03** (2016) 026 [arXiv:1512.02586] [INSPIRE].

JHEP09(2018)148

[73] CDF collaboration, T. Aaltonen et al., *Search for new particles decaying into dijets in proton-antiproton collisions at* $\sqrt{s} = 1.96$ *TeV*, *Phys. Rev.* **D 79** (2009) 112002 [arXiv:0812.4036] [INSPIRE].

[74] UA2 collaboration, J. Alitti et al., *A measurement of two jet decays of the W and Z bosons at the CERN* $\bar{p}p$ *collider*, *Z. Phys.* **C 49** (1991) 17 [INSPIRE].

[75] R.A. Fisher, *On the interpretation of* χ^2 *from contingency tables, and the calculation of p*, *J. Roy. Statist. Soc.* **85** (1922) 87.

[76] CMS collaboration, *Search for resonant production of high-mass photon pairs in proton-proton collisions at* $\sqrt{s} = 8$ *and* 13 *TeV*, *Phys. Rev. Lett.* **117** (2016) 051802 [arXiv:1606.04093] [INSPIRE].

[77] F. Garwood, *Fiducial limits for the Poisson distribution*, *Biometrika* **28** (1936) 437.

[78] M.J. Oreglia, *A study of the reactions* $\psi' \to \gamma\gamma\psi$, Ph.D. thesis, SLAC report SLAC-R-236, Stanford University, Stanford, CA, U.S.A., (1980) [INSPIRE].

[79] A.L. Read, *Linear interpolation of histograms*, *Nucl. Instrum. Meth.* **A 425** (1999) 357 [INSPIRE].

[80] CMS collaboration, *CMS luminosity measurements for the* 2016 *data taking period*, CMS-PAS-LUM-17-001, CERN, Geneva, Switzerland, (2017).

[81] J. Butterworth et al., *PDF4LHC recommendations for LHC run II*, *J. Phys.* **G 43** (2016) 023001 [arXiv:1510.03865] [INSPIRE].

[82] ATLAS collaboration, *Measurement of the inelastic proton-proton cross section at* $\sqrt{s} = 13$ *TeV with the ATLAS detector at the LHC*, *Phys. Rev. Lett.* **117** (2016) 182002 [arXiv:1606.02625] [INSPIRE].

[83] G. Cowan, K. Cranmer, E. Gross and O. Vitells, *Asymptotic formulae for likelihood-based tests of new physics*, *Eur. Phys. J.* **C 71** (2011) 1554 [*Erratum ibid.* **C 73** (2013) 2501] [arXiv:1007.1727] [INSPIRE].

[84] T. Junk, *Confidence level computation for combining searches with small statistics*, *Nucl. Instrum. Meth.* **A 434** (1999) 435 [hep-ex/9902006] [INSPIRE].

[85] A.L. Read, *Presentation of search results: the* CL_s *technique*, in *Durham IPPP Workshop: advanced statistical techniques in particle physics*, Durham, U.K., March 2002, pg. 2693 [*J. Phys.* **G 28** (2002) 2693] [INSPIRE].

[86] ATLAS and CMS collaborations and the LHC Higgs Combination Group, *Procedure for the LHC Higgs boson search combination in Summer* 2011, ATL-PHYS-PUB-2011-011, CERN, Geneva, Switzerland, (2011) [CMS-NOTE-2011-005].

[87] Particle Data Group collaboration, C. Patrignani et al., *Review of particle physics*, *Chin. Phys.* **C 40** (2016) 100001 [INSPIRE].

JHEP09(2018)148

The CMS collaboration

Yerevan Physics Institute, Yerevan, Armenia

A.M. Sirunyan, A. Tumasyan

Institut für Hochenergiephysik, Wien, Austria

W. Adam, F. Ambrogi, E. Asilar, T. Bergauer, J. Brandstetter, E. Brondolin, M. Dragicevic, J. Erö, A. Escalante Del Valle, M. Flechl, M. Friedl, R. Frühwirth[1], V.M. Ghete, J. Grossmann, J. Hrubec, M. Jeitler[1], A. König, N. Krammer, I. Krätschmer, D. Liko, T. Madlener, I. Mikulec, E. Pree, N. Rad, H. Rohringer, J. Schieck[1], R. Schöfbeck, M. Spanring, D. Spitzbart, W. Waltenberger, J. Wittmann, C.-E. Wulz[1], M. Zarucki

Institute for Nuclear Problems, Minsk, Belarus

V. Chekhovsky, V. Mossolov, J. Suarez Gonzalez

Universiteit Antwerpen, Antwerpen, Belgium

E.A. De Wolf, D. Di Croce, X. Janssen, J. Lauwers, M. Van De Klundert, H. Van Haevermaet, P. Van Mechelen, N. Van Remortel

Vrije Universiteit Brussel, Brussel, Belgium

S. Abu Zeid, F. Blekman, J. D'Hondt, I. De Bruyn, J. De Clercq, K. Deroover, G. Flouris, D. Lontkovskyi, S. Lowette, I. Marchesini, S. Moortgat, L. Moreels, Q. Python, K. Skovpen, S. Tavernier, W. Van Doninck, P. Van Mulders, I. Van Parijs

Université Libre de Bruxelles, Bruxelles, Belgium

D. Beghin, B. Bilin, H. Brun, B. Clerbaux, G. De Lentdecker, H. Delannoy, B. Dorney, G. Fasanella, L. Favart, R. Goldouzian, A. Grebenyuk, T. Lenzi, J. Luetic, T. Maerschalk, A. Marinov, T. Seva, E. Starling, C. Vander Velde, P. Vanlaer, D. Vannerom, R. Yonamine, F. Zenoni, F. Zhang[2]

Ghent University, Ghent, Belgium

A. Cimmino, T. Cornelis, D. Dobur, A. Fagot, M. Gul, I. Khvastunov[3], D. Poyraz, C. Roskas, S. Salva, M. Tytgat, W. Verbeke, N. Zaganidis

Université Catholique de Louvain, Louvain-la-Neuve, Belgium

H. Bakhshiansohi, O. Bondu, S. Brochet, G. Bruno, C. Caputo, A. Caudron, P. David, S. De Visscher, C. Delaere, M. Delcourt, B. Francois, A. Giammanco, M. Komm, G. Krintiras, V. Lemaitre, A. Magitteri, A. Mertens, M. Musich, K. Piotrzkowski, L. Quertenmont, A. Saggio, M. Vidal Marono, S. Wertz, J. Zobec

Centro Brasileiro de Pesquisas Fisicas, Rio de Janeiro, Brazil

W.L. Aldá Júnior, F.L. Alves, G.A. Alves, L. Brito, M. Correa Martins Junior, C. Hensel, A. Moraes, M.E. Pol, P. Rebello Teles

Universidade do Estado do Rio de Janeiro, Rio de Janeiro, Brazil

E. Belchior Batista Das Chagas, W. Carvalho, J. Chinellato[4], E. Coelho, E.M. Da Costa, G.G. Da Silveira[5], D. De Jesus Damiao, S. Fonseca De Souza, L.M. Huertas Guativa, H. Malbouisson, M. Melo De Almeida, C. Mora Herrera, L. Mundim, H. Nogima,

JHEP09(2018)148

L.J. Sanchez Rosas, A. Santoro, A. Sznajder, M. Thiel, E.J. Tonelli Manganote[4], F. Torres Da Silva De Araujo, A. Vilela Pereira

Universidade Estadual Paulista [a], Universidade Federal do ABC [b], São Paulo, Brazil

S. Ahuja[a], C.A. Bernardes[a], T.R. Fernandez Perez Tomei[a], E.M. Gregores[b], P.G. Mercadante[b], S.F. Novaes[a], Sandra S. Padula[a], D. Romero Abad[b], J.C. Ruiz Vargas[a]

Institute for Nuclear Research and Nuclear Energy, Bulgarian Academy of Sciences, Sofia, Bulgaria

A. Aleksandrov, R. Hadjiiska, P. Iaydjiev, M. Misheva, M. Rodozov, M. Shopova, G. Sultanov

University of Sofia, Sofia, Bulgaria

A. Dimitrov, L. Litov, B. Pavlov, P. Petkov

Beihang University, Beijing, China

W. Fang[6], X. Gao[6], L. Yuan

Institute of High Energy Physics, Beijing, China

M. Ahmad, J.G. Bian, G.M. Chen, H.S. Chen, M. Chen, Y. Chen, C.H. Jiang, D. Leggat, H. Liao, Z. Liu, F. Romeo, S.M. Shaheen, A. Spiezia, J. Tao, C. Wang, Z. Wang, E. Yazgan, H. Zhang, S. Zhang, J. Zhao

State Key Laboratory of Nuclear Physics and Technology, Peking University, Beijing, China

Y. Ban, G. Chen, J. Li, Q. Li, S. Liu, Y. Mao, S.J. Qian, D. Wang, Z. Xu

Tsinghua University, Beijing, China

Y. Wang

Universidad de Los Andes, Bogota, Colombia

C. Avila, A. Cabrera, C.A. Carrillo Montoya, L.F. Chaparro Sierra, C. Florez, C.F. González Hernández, J.D. Ruiz Alvarez, M.A. Segura Delgado

University of Split, Faculty of Electrical Engineering, Mechanical Engineering and Naval Architecture, Split, Croatia

B. Courbon, N. Godinovic, D. Lelas, I. Puljak, P.M. Ribeiro Cipriano, T. Sculac

University of Split, Faculty of Science, Split, Croatia

Z. Antunovic, M. Kovac

Institute Rudjer Boskovic, Zagreb, Croatia

V. Brigljevic, D. Ferencek, K. Kadija, B. Mesic, A. Starodumov[7], T. Susa

University of Cyprus, Nicosia, Cyprus

M.W. Ather, A. Attikis, G. Mavromanolakis, J. Mousa, C. Nicolaou, F. Ptochos, P.A. Razis, H. Rykaczewski

Charles University, Prague, Czech Republic

M. Finger[8], M. Finger Jr.[8]

JHEP09(2018)148

Universidad San Francisco de Quito, Quito, Ecuador
E. Carrera Jarrin

Academy of Scientific Research and Technology of the Arab Republic of Egypt, Egyptian Network of High Energy Physics, Cairo, Egypt
E. El-khateeb[9], S. Elgammal[10], A. Mohamed[11]

National Institute of Chemical Physics and Biophysics, Tallinn, Estonia
R.K. Dewanjee, M. Kadastik, L. Perrini, M. Raidal, A. Tiko, C. Veelken

Department of Physics, University of Helsinki, Helsinki, Finland
P. Eerola, H. Kirschenmann, J. Pekkanen, M. Voutilainen

Helsinki Institute of Physics, Helsinki, Finland
J. Havukainen, J.K. Heikkilä, T. Järvinen, V. Karimäki, R. Kinnunen, T. Lampén, K. Lassila-Perini, S. Laurila, S. Lehti, T. Lindén, P. Luukka, H. Siikonen, E. Tuominen, J. Tuominiemi

Lappeenranta University of Technology, Lappeenranta, Finland
T. Tuuva

IRFU, CEA, Université Paris-Saclay, Gif-sur-Yvette, France
M. Besancon, F. Couderc, M. Dejardin, D. Denegri, J.L. Faure, F. Ferri, S. Ganjour, S. Ghosh, P. Gras, G. Hamel de Monchenault, P. Jarry, I. Kucher, C. Leloup, E. Locci, M. Machet, J. Malcles, G. Negro, J. Rander, A. Rosowsky, M.Ö. Sahin, M. Titov

Laboratoire Leprince-Ringuet, Ecole polytechnique, CNRS/IN2P3, Université Paris-Saclay, Palaiseau, France
A. Abdulsalam, C. Amendola, I. Antropov, S. Baffioni, F. Beaudette, P. Busson, L. Cadamuro, C. Charlot, R. Granier de Cassagnac, M. Jo, S. Lisniak, A. Lobanov, J. Martin Blanco, M. Nguyen, C. Ochando, G. Ortona, P. Paganini, P. Pigard, R. Salerno, J.B. Sauvan, Y. Sirois, A.G. Stahl Leiton, T. Strebler, Y. Yilmaz, A. Zabi, A. Zghiche

Université de Strasbourg, CNRS, IPHC UMR 7178, F-67000 Strasbourg, France
J.-L. Agram[12], J. Andrea, D. Bloch, J.-M. Brom, M. Buttignol, E.C. Chabert, N. Chanon, C. Collard, E. Conte[12], X. Coubez, J.-C. Fontaine[12], D. Gelé, U. Goerlach, M. Jansová, A.-C. Le Bihan, N. Tonon, P. Van Hove

Centre de Calcul de l'Institut National de Physique Nucleaire et de Physique des Particules, CNRS/IN2P3, Villeurbanne, France
S. Gadrat

Université de Lyon, Université Claude Bernard Lyon 1, CNRS-IN2P3, Institut de Physique Nucléaire de Lyon, Villeurbanne, France
S. Beauceron, C. Bernet, G. Boudoul, R. Chierici, D. Contardo, P. Depasse, H. El Mamouni, J. Fay, L. Finco, S. Gascon, M. Gouzevitch, G. Grenier, B. Ille, F. Lagarde, I.B. Laktineh, M. Lethuillier, L. Mirabito, A.L. Pequegnot, S. Perries, A. Popov[13], V. Sordini, M. Vander Donckt, S. Viret

JHEP09(2018)148

Georgian Technical University, Tbilisi, Georgia
A. Khvedelidze[8]

Tbilisi State University, Tbilisi, Georgia
D. Lomidze

RWTH Aachen University, I. Physikalisches Institut, Aachen, Germany
C. Autermann, L. Feld, M.K. Kiesel, K. Klein, M. Lipinski, M. Preuten, C. Schomakers, J. Schulz, M. Teroerde, V. Zhukov[13]

RWTH Aachen University, III. Physikalisches Institut A, Aachen, Germany
A. Albert, E. Dietz-Laursonn, D. Duchardt, M. Endres, M. Erdmann, S. Erdweg, T. Esch, R. Fischer, A. Güth, M. Hamer, T. Hebbeker, C. Heidemann, K. Hoepfner, S. Knutzen, M. Merschmeyer, A. Meyer, P. Millet, S. Mukherjee, T. Pook, M. Radziej, H. Reithler, M. Rieger, F. Scheuch, D. Teyssier, S. Thüer

RWTH Aachen University, III. Physikalisches Institut B, Aachen, Germany
G. Flügge, B. Kargoll, T. Kress, A. Künsken, T. Müller, A. Nehrkorn, A. Nowack, C. Pistone, O. Pooth, A. Stahl[14]

Deutsches Elektronen-Synchrotron, Hamburg, Germany
M. Aldaya Martin, T. Arndt, C. Asawatangtrakuldee, K. Beernaert, O. Behnke, U. Behrens, A. Bermúdez Martínez, A.A. Bin Anuar, K. Borras[15], V. Botta, A. Campbell, P. Connor, C. Contreras-Campana, F. Costanza, C. Diez Pardos, G. Eckerlin, D. Eckstein, T. Eichhorn, E. Eren, E. Gallo[16], J. Garay Garcia, A. Geiser, J.M. Grados Luyando, A. Grohsjean, P. Gunnellini, M. Guthoff, A. Harb, J. Hauk, M. Hempel[17], H. Jung, M. Kasemann, J. Keaveney, C. Kleinwort, I. Korol, D. Krücker, W. Lange, A. Lelek, T. Lenz, J. Leonard, K. Lipka, W. Lohmann[17], R. Mankel, I.-A. Melzer-Pellmann, A.B. Meyer, G. Mittag, J. Mnich, A. Mussgiller, E. Ntomari, D. Pitzl, A. Raspereza, M. Savitskyi, P. Saxena, R. Shevchenko, S. Spannagel, N. Stefaniuk, G.P. Van Onsem, R. Walsh, Y. Wen, K. Wichmann, C. Wissing, O. Zenaiev

University of Hamburg, Hamburg, Germany
R. Aggleton, S. Bein, V. Blobel, M. Centis Vignali, T. Dreyer, E. Garutti, D. Gonzalez, J. Haller, A. Hinzmann, M. Hoffmann, A. Karavdina, R. Klanner, R. Kogler, N. Kovalchuk, S. Kurz, T. Lapsien, D. Marconi, M. Meyer, M. Niedziela, D. Nowatschin, F. Pantaleo[14], T. Peiffer, A. Perieanu, C. Scharf, P. Schleper, A. Schmidt, S. Schumann, J. Schwandt, J. Sonneveld, H. Stadie, G. Steinbrück, F.M. Stober, M. Stöver, H. Tholen, D. Troendle, E. Usai, A. Vanhoefer, B. Vormwald

Institut für Experimentelle Kernphysik, Karlsruhe, Germany
M. Akbiyik, C. Barth, M. Baselga, S. Baur, E. Butz, R. Caspart, T. Chwalek, F. Colombo, W. De Boer, A. Dierlamm, N. Faltermann, B. Freund, R. Friese, M. Giffels, M.A. Harrendorf, F. Hartmann[14], S.M. Heindl, U. Husemann, F. Kassel[14], S. Kudella, H. Mildner, M.U. Mozer, Th. Müller, M. Plagge, G. Quast, K. Rabbertz, M. Schröder, I. Shvetsov, G. Sieber, H.J. Simonis, R. Ulrich, S. Wayand, M. Weber, T. Weiler, S. Williamson, C. Wöhrmann, R. Wolf

JHEP09(2018)148

Institute of Nuclear and Particle Physics (INPP), NCSR Demokritos, Aghia Paraskevi, Greece
G. Anagnostou, G. Daskalakis, T. Geralis, A. Kyriakis, D. Loukas, I. Topsis-Giotis

National and Kapodistrian University of Athens, Athens, Greece
G. Karathanasis, S. Kesisoglou, A. Panagiotou, N. Saoulidou

National Technical University of Athens, Athens, Greece
K. Kousouris

University of Ioánnina, Ioánnina, Greece
I. Evangelou, C. Foudas, P. Gianneios, P. Katsoulis, P. Kokkas, S. Mallios, N. Manthos, I. Papadopoulos, E. Paradas, J. Strologas, F.A. Triantis, D. Tsitsonis

MTA-ELTE Lendület CMS Particle and Nuclear Physics Group, Eötvös Loránd University, Budapest, Hungary
M. Csanad, N. Filipovic, G. Pasztor, O. Surányi, G.I. Veres[18]

Wigner Research Centre for Physics, Budapest, Hungary
G. Bencze, C. Hajdu, D. Horvath[19], Á. Hunyadi, F. Sikler, V. Veszpremi

Institute of Nuclear Research ATOMKI, Debrecen, Hungary
N. Beni, S. Czellar, J. Karancsi[20], A. Makovec, J. Molnar, Z. Szillasi

Institute of Physics, University of Debrecen, Debrecen, Hungary
M. Bartók[18], P. Raics, Z.L. Trocsanyi, B. Ujvari

Indian Institute of Science (IISc), Bangalore, India
S. Choudhury, J.R. Komaragiri

National Institute of Science Education and Research, Bhubaneswar, India
S. Bahinipati[21], S. Bhowmik, P. Mal, K. Mandal, A. Nayak[22], D.K. Sahoo[21], N. Sahoo, S.K. Swain

Panjab University, Chandigarh, India
S. Bansal, S.B. Beri, V. Bhatnagar, R. Chawla, N. Dhingra, A.K. Kalsi, A. Kaur, M. Kaur, S. Kaur, R. Kumar, P. Kumari, A. Mehta, J.B. Singh, G. Walia

University of Delhi, Delhi, India
A. Bhardwaj, S. Chauhan, B.C. Choudhary, R.B. Garg, S. Keshri, A. Kumar, Ashok Kumar, S. Malhotra, M. Naimuddin, K. Ranjan, Aashaq Shah, R. Sharma

Saha Institute of Nuclear Physics, HBNI, Kolkata, India
R. Bhardwaj, R. Bhattacharya, S. Bhattacharya, U. Bhawandeep, S. Dey, S. Dutt, S. Dutta, S. Ghosh, N. Majumdar, A. Modak, K. Mondal, S. Mukhopadhyay, S. Nandan, A. Purohit, A. Roy, S. Roy Chowdhury, S. Sarkar, M. Sharan, S. Thakur

Indian Institute of Technology Madras, Madras, India
P.K. Behera

JHEP09(2018)148

Bhabha Atomic Research Centre, Mumbai, India

R. Chudasama, D. Dutta, V. Jha, V. Kumar, A.K. Mohanty[14], P.K. Netrakanti, L.M. Pant, P. Shukla, A. Topkar

Tata Institute of Fundamental Research-A, Mumbai, India

T. Aziz, S. Dugad, B. Mahakud, S. Mitra, G.B. Mohanty, N. Sur, B. Sutar

Tata Institute of Fundamental Research-B, Mumbai, India

S. Banerjee, S. Bhattacharya, S. Chatterjee, P. Das, M. Guchait, Sa. Jain, S. Kumar, M. Maity[23], G. Majumder, K. Mazumdar, T. Sarkar[23], N. Wickramage[24]

Indian Institute of Science Education and Research (IISER), Pune, India

S. Chauhan, S. Dube, V. Hegde, A. Kapoor, K. Kothekar, S. Pandey, A. Rane, S. Sharma

Institute for Research in Fundamental Sciences (IPM), Tehran, Iran

S. Chenarani[25], E. Eskandari Tadavani, S.M. Etesami[25], M. Khakzad, M. Mohammadi Najafabadi, M. Naseri, S. Paktinat Mehdiabadi[26], F. Rezaei Hosseinabadi, B. Safarzadeh[27], M. Zeinali

University College Dublin, Dublin, Ireland

M. Felcini, M. Grunewald

INFN Sezione di Bari [a], Università di Bari [b], Politecnico di Bari [c], Bari, Italy

M. Abbrescia[a,b], C. Calabria[a,b], A. Colaleo[a], D. Creanza[a,c], L. Cristella[a,b], N. De Filippis[a,c], M. De Palma[a,b], F. Errico[a,b], L. Fiore[a], G. Iaselli[a,c], S. Lezki[a,b], G. Maggi[a,c], M. Maggi[a], G. Miniello[a,b], S. My[a,b], S. Nuzzo[a,b], A. Pompili[a,b], G. Pugliese[a,c], R. Radogna[a], A. Ranieri[a], G. Selvaggi[a,b], A. Sharma[a], L. Silvestris[a,14], R. Venditti[a], P. Verwilligen[a]

INFN Sezione di Bologna [a], Università di Bologna [b], Bologna, Italy

G. Abbiendi[a], C. Battilana[a,b], D. Bonacorsi[a,b], L. Borgonovi[a,b], S. Braibant-Giacomelli[a,b], R. Campanini[a,b], P. Capiluppi[a,b], A. Castro[a,b], F.R. Cavallo[a], S.S. Chhibra[a], G. Codispoti[a,b], M. Cuffiani[a,b], G.M. Dallavalle[a], F. Fabbri[a], A. Fanfani[a,b], D. Fasanella[a,b], P. Giacomelli[a], C. Grandi[a], L. Guiducci[a,b], S. Marcellini[a], G. Masetti[a], A. Montanari[a], F.L. Navarria[a,b], A. Perrotta[a], A.M. Rossi[a,b], T. Rovelli[a,b], G.P. Siroli[a,b], N. Tosi[a]

INFN Sezione di Catania [a], Università di Catania [b], Catania, Italy

S. Albergo[a,b], S. Costa[a,b], A. Di Mattia[a], F. Giordano[a,b], R. Potenza[a,b], A. Tricomi[a,b], C. Tuve[a,b]

INFN Sezione di Firenze [a], Università di Firenze [b], Firenze, Italy

G. Barbagli[a], K. Chatterjee[a,b], V. Ciulli[a,b], C. Civinini[a], R. D'Alessandro[a,b], E. Focardi[a,b], P. Lenzi[a,b], M. Meschini[a], S. Paoletti[a], L. Russo[a,28], G. Sguazzoni[a], D. Strom[a], L. Viliani[a,b,14]

INFN Laboratori Nazionali di Frascati, Frascati, Italy

L. Benussi, S. Bianco, F. Fabbri, D. Piccolo, F. Primavera[14]

JHEP09(2018)148

INFN Sezione di Genova [a], Università di Genova [b], Genova, Italy
V. Calvelli[a,b], F. Ferro[a], F. Ravera[a,b], E. Robutti[a], S. Tosi[a,b]

INFN Sezione di Milano-Bicocca [a], Università di Milano-Bicocca [b], Milano, Italy
A. Benaglia[a], A. Beschi[b], L. Brianza[a,b], F. Brivio[a,b], V. Ciriolo[a,b,14], M.E. Dinardo[a,b], S. Fiorendi[a,b], S. Gennai[a], A. Ghezzi[a,b], P. Govoni[a,b], M. Malberti[a,b], S. Malvezzi[a], R.A. Manzoni[a,b], D. Menasce[a], L. Moroni[a], M. Paganoni[a,b], K. Pauwels[a,b], D. Pedrini[a], S. Pigazzini[a,b,29], S. Ragazzi[a,b], T. Tabarelli de Fatis[a,b]

INFN Sezione di Napoli [a], Università di Napoli 'Federico II' [b], Napoli, Italy, Università della Basilicata [c], Potenza, Italy, Università G. Marconi [d], Roma, Italy
S. Buontempo[a], N. Cavallo[a,c], S. Di Guida[a,d,14], F. Fabozzi[a,c], F. Fienga[a,b], A.O.M. Iorio[a,b], W.A. Khan[a], L. Lista[a], S. Meola[a,d,14], P. Paolucci[a,14], C. Sciacca[a,b], F. Thyssen[a]

INFN Sezione di Padova [a], Università di Padova [b], Padova, Italy, Università di Trento [c], Trento, Italy
P. Azzi[a], N. Bacchetta[a], L. Benato[a,b], A. Boletti[a,b], R. Carlin[a,b], A. Carvalho Antunes De Oliveira[a,b], M. Dall'Osso[a,b], P. De Castro Manzano[a], T. Dorigo[a], U. Dosselli[a], S. Fantinel[a], U. Gasparini[a,b], A. Gozzelino[a], S. Lacaprara[a], P. Lujan, M. Margoni[a,b], A.T. Meneguzzo[a,b], N. Pozzobon[a,b], P. Ronchese[a,b], R. Rossin[a,b], F. Simonetto[a,b], E. Torassa[a], S. Ventura[a], M. Zanetti[a,b], P. Zotto[a,b], G. Zumerle[a,b]

INFN Sezione di Pavia [a], Università di Pavia [b], Pavia, Italy
A. Braghieri[a], A. Magnani[a], P. Montagna[a,b], S.P. Ratti[a,b], V. Re[a], M. Ressegotti[a,b], C. Riccardi[a,b], P. Salvini[a], I. Vai[a,b], P. Vitulo[a,b]

INFN Sezione di Perugia [a], Università di Perugia [b], Perugia, Italy
L. Alunni Solestizi[a,b], M. Biasini[a,b], G.M. Bilei[a], C. Cecchi[a,b], D. Ciangottini[a,b], L. Fanò[a,b], R. Leonardi[a,b], E. Manoni[a], G. Mantovani[a,b], V. Mariani[a,b], M. Menichelli[a], A. Rossi[a,b], A. Santocchia[a,b], D. Spiga[a]

INFN Sezione di Pisa [a], Università di Pisa [b], Scuola Normale Superiore di Pisa [c], Pisa, Italy
K. Androsov[a], P. Azzurri[a,14], G. Bagliesi[a], T. Boccali[a], L. Borrello, R. Castaldi[a], M.A. Ciocci[a,b], R. Dell'Orso[a], G. Fedi[a], L. Giannini[a,c], A. Giassi[a], M.T. Grippo[a,28], F. Ligabue[a,c], T. Lomtadze[a], E. Manca[a,c], G. Mandorli[a,c], A. Messineo[a,b], F. Palla[a], A. Rizzi[a,b], A. Savoy-Navarro[a,30], P. Spagnolo[a], R. Tenchini[a], G. Tonelli[a,b], A. Venturi[a], P.G. Verdini[a]

INFN Sezione di Roma [a], Sapienza Università di Roma [b], Rome, Italy
L. Barone[a,b], F. Cavallari[a], M. Cipriani[a,b], N. Daci[a], D. Del Re[a,b,14], E. Di Marco[a,b], M. Diemoz[a], S. Gelli[a,b], E. Longo[a,b], F. Margaroli[a,b], B. Marzocchi[a,b], P. Meridiani[a], G. Organtini[a,b], R. Paramatti[a,b], F. Preiato[a,b], S. Rahatlou[a,b], C. Rovelli[a], F. Santanastasio[a,b]

JHEP09(2018)148

INFN Sezione di Torino [a], Università di Torino [b], Torino, Italy, Università del Piemonte Orientale [c], Novara, Italy

N. Amapane[a,b], R. Arcidiacono[a,c], S. Argiro[a,b], M. Arneodo[a,c], N. Bartosik[a], R. Bellan[a,b], C. Biino[a], N. Cartiglia[a], F. Cenna[a,b], M. Costa[a,b], R. Covarelli[a,b], A. Degano[a,b], N. Demaria[a], B. Kiani[a,b], C. Mariotti[a], S. Maselli[a], E. Migliore[a,b], V. Monaco[a,b], E. Monteil[a,b], M. Monteno[a], M.M. Obertino[a,b], L. Pacher[a,b], N. Pastrone[a], M. Pelliccioni[a], G.L. Pinna Angioni[a,b], A. Romero[a,b], M. Ruspa[a,c], R. Sacchi[a,b], K. Shchelina[a,b], V. Sola[a], A. Solano[a,b], A. Staiano[a], P. Traczyk[a,b]

INFN Sezione di Trieste [a], Università di Trieste [b], Trieste, Italy

S. Belforte[a], M. Casarsa[a], F. Cossutti[a], G. Della Ricca[a,b], A. Zanetti[a]

Kyungpook National University, Daegu, Korea

D.H. Kim, G.N. Kim, M.S. Kim, J. Lee, S. Lee, S.W. Lee, C.S. Moon, Y.D. Oh, S. Sekmen, D.C. Son, Y.C. Yang

Chonbuk National University, Jeonju, Korea

A. Lee

Chonnam National University, Institute for Universe and Elementary Particles, Kwangju, Korea

H. Kim, D.H. Moon, G. Oh

Hanyang University, Seoul, Korea

J.A. Brochero Cifuentes, J. Goh, T.J. Kim

Korea University, Seoul, Korea

S. Cho, S. Choi, Y. Go, D. Gyun, S. Ha, B. Hong, Y. Jo, Y. Kim, K. Lee, K.S. Lee, S. Lee, J. Lim, S.K. Park, Y. Roh

Seoul National University, Seoul, Korea

J. Almond, J. Kim, J.S. Kim, H. Lee, K. Lee, K. Nam, S.B. Oh, B.C. Radburn-Smith, S.h. Seo, U.K. Yang, H.D. Yoo, G.B. Yu

University of Seoul, Seoul, Korea

H. Kim, J.H. Kim, J.S.H. Lee, I.C. Park

Sungkyunkwan University, Suwon, Korea

Y. Choi, C. Hwang, J. Lee, I. Yu

Vilnius University, Vilnius, Lithuania

V. Dudenas, A. Juodagalvis, J. Vaitkus

National Centre for Particle Physics, Universiti Malaya, Kuala Lumpur, Malaysia

I. Ahmed, Z.A. Ibrahim, M.A.B. Md Ali[31], F. Mohamad Idris[32], W.A.T. Wan Abdullah, M.N. Yusli, Z. Zolkapli

JHEP09(2018)148

Centro de Investigacion y de Estudios Avanzados del IPN, Mexico City, Mexico

Duran-Osuna, M. C., H. Castilla-Valdez, E. De La Cruz-Burelo, Ramirez-Sanchez, G., I. Heredia-De La Cruz[33], Rabadan-Trejo, R. I., R. Lopez-Fernandez, J. Mejia Guisao, Reyes-Almanza, R, A. Sanchez-Hernandez

Universidad Iberoamericana, Mexico City, Mexico

S. Carrillo Moreno, C. Oropeza Barrera, F. Vazquez Valencia

Benemerita Universidad Autonoma de Puebla, Puebla, Mexico

J. Eysermans, I. Pedraza, H.A. Salazar Ibarguen, C. Uribe Estrada

Universidad Autónoma de San Luis Potosí, San Luis Potosí, Mexico

A. Morelos Pineda

University of Auckland, Auckland, New Zealand

D. Krofcheck

University of Canterbury, Christchurch, New Zealand

P.H. Butler

National Centre for Physics, Quaid-I-Azam University, Islamabad, Pakistan

A. Ahmad, M. Ahmad, Q. Hassan, H.R. Hoorani, A. Saddique, M.A. Shah, M. Shoaib, M. Waqas

National Centre for Nuclear Research, Swierk, Poland

H. Bialkowska, M. Bluj, B. Boimska, T. Frueboes, M. Górski, M. Kazana, K. Nawrocki, M. Szleper, P. Zalewski

Institute of Experimental Physics, Faculty of Physics, University of Warsaw, Warsaw, Poland

K. Bunkowski, A. Byszuk[34], K. Doroba, A. Kalinowski, M. Konecki, J. Krolikowski, M. Misiura, M. Olszewski, A. Pyskir, M. Walczak

Laboratório de Instrumentação e Física Experimental de Partículas, Lisboa, Portugal

P. Bargassa, C. Beirão Da Cruz E Silva, A. Di Francesco, P. Faccioli, B. Galinhas, M. Gallinaro, J. Hollar, N. Leonardo, L. Lloret Iglesias, M.V. Nemallapudi, J. Seixas, G. Strong, O. Toldaiev, D. Vadruccio, J. Varela

Joint Institute for Nuclear Research, Dubna, Russia

V. Alexakhin, P. Bunin, M. Gavrilenko, A. Golunov, I. Golutvin, N. Gorbounov, A. Kamenev, V. Karjavin, A. Lanev, A. Malakhov, V. Matveev[35,36], V. Palichik, V. Perelygin, M. Savina, S. Shmatov, S. Shulha, V. Smirnov, A. Zarubin

Petersburg Nuclear Physics Institute, Gatchina (St. Petersburg), Russia

Y. Ivanov, V. Kim[37], E. Kuznetsova[38], P. Levchenko, V. Murzin, V. Oreshkin, I. Smirnov, D. Sosnov, V. Sulimov, L. Uvarov, S. Vavilov, A. Vorobyev

JHEP09(2018)148

Institute for Nuclear Research, Moscow, Russia

Yu. Andreev, A. Dermenev, S. Gninenko, N. Golubev, A. Karneyeu, M. Kirsanov, N. Krasnikov, A. Pashenkov, D. Tlisov, A. Toropin

Institute for Theoretical and Experimental Physics, Moscow, Russia

V. Epshteyn, V. Gavrilov, N. Lychkovskaya, V. Popov, I. Pozdnyakov, G. Safronov, A. Spiridonov, A. Stepennov, M. Toms, E. Vlasov, A. Zhokin

Moscow Institute of Physics and Technology, Moscow, Russia

T. Aushev, A. Bylinkin[36]

National Research Nuclear University 'Moscow Engineering Physics Institute' (MEPhI), Moscow, Russia

M. Chadeeva[39], P. Parygin, D. Philippov, S. Polikarpov, E. Popova, V. Rusinov

P.N. Lebedev Physical Institute, Moscow, Russia

V. Andreev, M. Azarkin[36], I. Dremin[36], M. Kirakosyan[36], A. Terkulov

Skobeltsyn Institute of Nuclear Physics, Lomonosov Moscow State University, Moscow, Russia

A. Baskakov, A. Belyaev, E. Boos, V. Bunichev, M. Dubinin[40], L. Dudko, A. Ershov, V. Klyukhin, O. Kodolova, I. Lokhtin, I. Miagkov, S. Obraztsov, M. Perfilov, S. Petrushanko, V. Savrin

Novosibirsk State University (NSU), Novosibirsk, Russia

V. Blinov[41], D. Shtol[41], Y. Skovpen[41]

State Research Center of Russian Federation, Institute for High Energy Physics, Protvino, Russia

I. Azhgirey, I. Bayshev, S. Bitioukov, D. Elumakhov, A. Godizov, V. Kachanov, A. Kalinin, D. Konstantinov, P. Mandrik, V. Petrov, R. Ryutin, A. Sobol, S. Troshin, N. Tyurin, A. Uzunian, A. Volkov

University of Belgrade, Faculty of Physics and Vinca Institute of Nuclear Sciences, Belgrade, Serbia

P. Adzic[42], P. Cirkovic, D. Devetak, M. Dordevic, J. Milosevic, V. Rekovic

Centro de Investigaciones Energéticas Medioambientales y Tecnológicas (CIEMAT), Madrid, Spain

J. Alcaraz Maestre, A. Álvarez Fernández, I. Bachiller, M. Barrio Luna, M. Cerrada, N. Colino, B. De La Cruz, A. Delgado Peris, C. Fernandez Bedoya, J.P. Fernández Ramos, J. Flix, M.C. Fouz, O. Gonzalez Lopez, S. Goy Lopez, J.M. Hernandez, M.I. Josa, D. Moran, A. Pérez-Calero Yzquierdo, J. Puerta Pelayo, A. Quintario Olmeda, I. Redondo, L. Romero, M.S. Soares

Universidad Autónoma de Madrid, Madrid, Spain

C. Albajar, J.F. de Trocóniz, M. Missiroli

JHEP09(2018)148

Universidad de Oviedo, Oviedo, Spain

J. Cuevas, C. Erice, J. Fernandez Menendez, I. Gonzalez Caballero, J.R. González Fernández, E. Palencia Cortezon, S. Sanchez Cruz, P. Vischia, J.M. Vizan Garcia

Instituto de Física de Cantabria (IFCA), CSIC-Universidad de Cantabria, Santander, Spain

I.J. Cabrillo, A. Calderon, B. Chazin Quero, E. Curras, J. Duarte Campderros, M. Fernandez, J. Garcia-Ferrero, G. Gomez, A. Lopez Virto, J. Marco, C. Martinez Rivero, P. Martinez Ruiz del Arbol, F. Matorras, J. Piedra Gomez, T. Rodrigo, A. Ruiz-Jimeno, L. Scodellaro, N. Trevisani, I. Vila, R. Vilar Cortabitarte

CERN, European Organization for Nuclear Research, Geneva, Switzerland

D. Abbaneo, B. Akgun, E. Auffray, P. Baillon, A.H. Ball, D. Barney, J. Bendavid, M. Bianco, P. Bloch, A. Bocci, C. Botta, T. Camporesi, R. Castello, M. Cepeda, G. Cerminara, E. Chapon, Y. Chen, D. d'Enterria, A. Dabrowski, V. Daponte, A. David, M. De Gruttola, A. De Roeck, N. Deelen, M. Dobson, T. du Pree, M. Dünser, N. Dupont, A. Elliott-Peisert, P. Everaerts, F. Fallavollita, G. Franzoni, J. Fulcher, W. Funk, D. Gigi, A. Gilbert, K. Gill, F. Glege, D. Gulhan, P. Harris, J. Hegeman, V. Innocente, A. Jafari, P. Janot, O. Karacheban[17], J. Kieseler, V. Knünz, A. Kornmayer, M.J. Kortelainen, M. Krammer[1], C. Lange, P. Lecoq, C. Lourenço, M.T. Lucchini, L. Malgeri, M. Mannelli, A. Martelli, F. Meijers, J.A. Merlin, S. Mersi, E. Meschi, P. Milenovic[43], F. Moortgat, M. Mulders, H. Neugebauer, J. Ngadiuba, S. Orfanelli, L. Orsini, L. Pape, E. Perez, M. Peruzzi, A. Petrilli, G. Petrucciani, A. Pfeiffer, M. Pierini, D. Rabady, A. Racz, T. Reis, G. Rolandi[44], M. Rovere, H. Sakulin, C. Schäfer, C. Schwick, M. Seidel, M. Selvaggi, A. Sharma, P. Silva, P. Sphicas[45], A. Stakia, J. Steggemann, M. Stoye, M. Tosi, D. Treille, A. Triossi, A. Tsirou, V. Veckalns[46], M. Verweij, W.D. Zeuner

Paul Scherrer Institut, Villigen, Switzerland

W. Bertl†, L. Caminada[47], K. Deiters, W. Erdmann, R. Horisberger, Q. Ingram, H.C. Kaestli, D. Kotlinski, U. Langenegger, T. Rohe, S.A. Wiederkehr

ETH Zurich - Institute for Particle Physics and Astrophysics (IPA), Zurich, Switzerland

M. Backhaus, L. Bäni, P. Berger, L. Bianchini, B. Casal, G. Dissertori, M. Dittmar, M. Donegà, C. Dorfer, C. Grab, C. Heidegger, D. Hits, J. Hoss, G. Kasieczka, T. Klijnsma, W. Lustermann, B. Mangano, M. Marionneau, M.T. Meinhard, D. Meister, F. Micheli, P. Musella, F. Nessi-Tedaldi, F. Pandolfi, J. Pata, F. Pauss, G. Perrin, L. Perrozzi, M. Quittnat, M. Reichmann, D.A. Sanz Becerra, M. Schönenberger, L. Shchutska, V.R. Tavolaro, K. Theofilatos, M.L. Vesterbacka Olsson, R. Wallny, D.H. Zhu

Universität Zürich, Zurich, Switzerland

T.K. Aarrestad, C. Amsler[48], M.F. Canelli, A. De Cosa, R. Del Burgo, S. Donato, C. Galloni, T. Hreus, B. Kilminster, D. Pinna, G. Rauco, P. Robmann, D. Salerno, K. Schweiger, C. Seitz, Y. Takahashi, A. Zucchetta

JHEP09(2018)148

National Central University, Chung-Li, Taiwan
V. Candelise, Y.H. Chang, K.y. Cheng, T.H. Doan, Sh. Jain, R. Khurana, C.M. Kuo, W. Lin, A. Pozdnyakov, S.S. Yu

National Taiwan University (NTU), Taipei, Taiwan
P. Chang, Y. Chao, K.F. Chen, P.H. Chen, F. Fiori, W.-S. Hou, Y. Hsiung, Arun Kumar, Y.F. Liu, R.-S. Lu, E. Paganis, A. Psallidas, A. Steen, J.f. Tsai

Chulalongkorn University, Faculty of Science, Department of Physics, Bangkok, Thailand
B. Asavapibhop, K. Kovitanggoon, G. Singh, N. Srimanobhas

Çukurova University, Physics Department, Science and Art Faculty, Adana, Turkey
A. Bat, F. Boran, S. Damarseckin, Z.S. Demiroglu, C. Dozen, E. Eskut, S. Girgis, G. Gokbulut, Y. Guler, I. Hos[49], E.E. Kangal[50], O. Kara, U. Kiminsu, M. Oglakci, G. Onengut[51], K. Ozdemir[52], S. Ozturk[53], A. Polatoz, D. Sunar Cerci[54], U.G. Tok, H. Topakli[53], S. Turkcapar, I.S. Zorbakir, C. Zorbilmez

Middle East Technical University, Physics Department, Ankara, Turkey
G. Karapinar[55], K. Ocalan[56], M. Yalvac, M. Zeyrek

Bogazici University, Istanbul, Turkey
E. Gülmez, M. Kaya[57], O. Kaya[58], S. Tekten, E.A. Yetkin[59]

Istanbul Technical University, Istanbul, Turkey
M.N. Agaras, S. Atay, A. Cakir, K. Cankocak, I. Köseoglu

Institute for Scintillation Materials of National Academy of Science of Ukraine, Kharkov, Ukraine
B. Grynyov

National Scientific Center, Kharkov Institute of Physics and Technology, Kharkov, Ukraine
L. Levchuk

University of Bristol, Bristol, United Kingdom
F. Ball, L. Beck, J.J. Brooke, D. Burns, E. Clement, D. Cussans, O. Davignon, H. Flacher, J. Goldstein, G.P. Heath, H.F. Heath, L. Kreczko, D.M. Newbold[60], S. Paramesvaran, T. Sakuma, S. Seif El Nasr-storey, D. Smith, V.J. Smith

Rutherford Appleton Laboratory, Didcot, United Kingdom
K.W. Bell, A. Belyaev[61], C. Brew, R.M. Brown, L. Calligaris, D. Cieri, D.J.A. Cockerill, J.A. Coughlan, K. Harder, S. Harper, J. Linacre, E. Olaiya, D. Petyt, C.H. Shepherd-Themistocleous, A. Thea, I.R. Tomalin, T. Williams

Imperial College, London, United Kingdom
G. Auzinger, R. Bainbridge, J. Borg, S. Breeze, O. Buchmuller, A. Bundock, S. Casasso, M. Citron, D. Colling, L. Corpe, P. Dauncey, G. Davies, A. De Wit, M. Della Negra,

JHEP09(2018)148

R. Di Maria, A. Elwood, Y. Haddad, G. Hall, G. Iles, T. James, R. Lane, C. Laner, L. Lyons, A.-M. Magnan, S. Malik, L. Mastrolorenzo, T. Matsushita, J. Nash, A. Nikitenko[7], V. Palladino, M. Pesaresi, D.M. Raymond, A. Richards, A. Rose, E. Scott, C. Seez, A. Shtipliyski, S. Summers, A. Tapper, K. Uchida, M. Vazquez Acosta[62], T. Virdee[14], N. Wardle, D. Winterbottom, J. Wright, S.C. Zenz

Brunel University, Uxbridge, United Kingdom

J.E. Cole, P.R. Hobson, A. Khan, P. Kyberd, I.D. Reid, L. Teodorescu, S. Zahid

Baylor University, Waco, U.S.A.

A. Borzou, K. Call, J. Dittmann, K. Hatakeyama, H. Liu, N. Pastika, C. Smith

Catholic University of America, Washington DC, U.S.A.

R. Bartek, A. Dominguez

The University of Alabama, Tuscaloosa, U.S.A.

A. Buccilli, S.I. Cooper, C. Henderson, P. Rumerio, C. West

Boston University, Boston, U.S.A.

D. Arcaro, A. Avetisyan, T. Bose, D. Gastler, D. Rankin, C. Richardson, J. Rohlf, L. Sulak, D. Zou

Brown University, Providence, U.S.A.

G. Benelli, D. Cutts, A. Garabedian, M. Hadley, J. Hakala, U. Heintz, J.M. Hogan, K.H.M. Kwok, E. Laird, G. Landsberg, J. Lee, Z. Mao, M. Narain, J. Pazzini, S. Piperov, S. Sagir, R. Syarif, D. Yu

University of California, Davis, Davis, U.S.A.

R. Band, C. Brainerd, R. Breedon, D. Burns, M. Calderon De La Barca Sanchez, M. Chertok, J. Conway, R. Conway, P.T. Cox, R. Erbacher, C. Flores, G. Funk, W. Ko, R. Lander, C. Mclean, M. Mulhearn, D. Pellett, J. Pilot, S. Shalhout, M. Shi, J. Smith, D. Stolp, K. Tos, M. Tripathi, Z. Wang

University of California, Los Angeles, U.S.A.

M. Bachtis, C. Bravo, R. Cousins, A. Dasgupta, A. Florent, J. Hauser, M. Ignatenko, N. Mccoll, S. Regnard, D. Saltzberg, C. Schnaible, V. Valuev

University of California, Riverside, Riverside, U.S.A.

E. Bouvier, K. Burt, R. Clare, J. Ellison, J.W. Gary, S.M.A. Ghiasi Shirazi, G. Hanson, J. Heilman, G. Karapostoli, E. Kennedy, F. Lacroix, O.R. Long, M. Olmedo Negrete, M.I. Paneva, W. Si, L. Wang, H. Wei, S. Wimpenny, B. R. Yates

University of California, San Diego, La Jolla, U.S.A.

J.G. Branson, S. Cittolin, M. Derdzinski, R. Gerosa, D. Gilbert, B. Hashemi, A. Holzner, D. Klein, G. Kole, V. Krutelyov, J. Letts, M. Masciovecchio, D. Olivito, S. Padhi, M. Pieri, M. Sani, V. Sharma, M. Tadel, A. Vartak, S. Wasserbaech[63], J. Wood, F. Würthwein, A. Yagil, G. Zevi Della Porta

JHEP09(2018)148

University of California, Santa Barbara - Department of Physics, Santa Barbara, U.S.A.

N. Amin, R. Bhandari, J. Bradmiller-Feld, C. Campagnari, A. Dishaw, V. Dutta, M. Franco Sevilla, F. Golf, L. Gouskos, R. Heller, J. Incandela, A. Ovcharova, H. Qu, J. Richman, D. Stuart, I. Suarez, J. Yoo

California Institute of Technology, Pasadena, U.S.A.

D. Anderson, A. Bornheim, J.M. Lawhorn, H.B. Newman, T. Nguyen, C. Pena, M. Spiropulu, J.R. Vlimant, S. Xie, Z. Zhang, R.Y. Zhu

Carnegie Mellon University, Pittsburgh, U.S.A.

M.B. Andrews, T. Ferguson, T. Mudholkar, M. Paulini, J. Russ, M. Sun, H. Vogel, I. Vorobiev, M. Weinberg

University of Colorado Boulder, Boulder, U.S.A.

J.P. Cumalat, W.T. Ford, F. Jensen, A. Johnson, M. Krohn, S. Leontsinis, T. Mulholland, K. Stenson, S.R. Wagner

Cornell University, Ithaca, U.S.A.

J. Alexander, J. Chaves, J. Chu, S. Dittmer, K. Mcdermott, N. Mirman, J.R. Patterson, D. Quach, A. Rinkevicius, A. Ryd, L. Skinnari, L. Soffi, S.M. Tan, Z. Tao, J. Thom, J. Tucker, P. Wittich, M. Zientek

Fermi National Accelerator Laboratory, Batavia, U.S.A.

S. Abdullin, M. Albrow, M. Alyari, G. Apollinari, A. Apresyan, A. Apyan, S. Banerjee, L.A.T. Bauerdick, A. Beretvas, J. Berryhill, P.C. Bhat, G. Bolla[†], K. Burkett, J.N. Butler, A. Canepa, G.B. Cerati, H.W.K. Cheung, F. Chlebana, M. Cremonesi, J. Duarte, V.D. Elvira, J. Freeman, Z. Gecse, E. Gottschalk, L. Gray, D. Green, S. Grünendahl, O. Gutsche, R.M. Harris, S. Hasegawa, J. Hirschauer, Z. Hu, B. Jayatilaka, S. Jindariani, M. Johnson, U. Joshi, B. Klima, B. Kreis, S. Lammel, D. Lincoln, R. Lipton, M. Liu, T. Liu, R. Lopes De Sá, J. Lykken, K. Maeshima, N. Magini, J.M. Marraffino, D. Mason, P. McBride, P. Merkel, S. Mrenna, S. Nahn, V. O'Dell, K. Pedro, O. Prokofyev, G. Rakness, L. Ristori, B. Schneider, E. Sexton-Kennedy, A. Soha, W.J. Spalding, L. Spiegel, S. Stoynev, J. Strait, N. Strobbe, L. Taylor, S. Tkaczyk, N.V. Tran, L. Uplegger, E.W. Vaandering, C. Vernieri, M. Verzocchi, R. Vidal, M. Wang, H.A. Weber, A. Whitbeck

University of Florida, Gainesville, U.S.A.

D. Acosta, P. Avery, P. Bortignon, D. Bourilkov, A. Brinkerhoff, A. Carnes, M. Carver, D. Curry, R.D. Field, I.K. Furic, S.V. Gleyzer, B.M. Joshi, J. Konigsberg, A. Korytov, K. Kotov, P. Ma, K. Matchev, H. Mei, G. Mitselmakher, K. Shi, D. Sperka, N. Terentyev, L. Thomas, J. Wang, S. Wang, J. Yelton

Florida International University, Miami, U.S.A.

Y.R. Joshi, S. Linn, P. Markowitz, J.L. Rodriguez

Florida State University, Tallahassee, U.S.A.

A. Ackert, T. Adams, A. Askew, S. Hagopian, V. Hagopian, K.F. Johnson, T. Kolberg, G. Martinez, T. Perry, H. Prosper, A. Saha, A. Santra, V. Sharma, R. Yohay

JHEP09(2018)148

Florida Institute of Technology, Melbourne, U.S.A.

M.M. Baarmand, V. Bhopatkar, S. Colafranceschi, M. Hohlmann, D. Noonan, T. Roy, F. Yumiceva

University of Illinois at Chicago (UIC), Chicago, U.S.A.

M.R. Adams, L. Apanasevich, D. Berry, R.R. Betts, R. Cavanaugh, X. Chen, O. Evdokimov, C.E. Gerber, D.A. Hangal, D.J. Hofman, K. Jung, J. Kamin, I.D. Sandoval Gonzalez, M.B. Tonjes, H. Trauger, N. Varelas, H. Wang, Z. Wu, J. Zhang

The University of Iowa, Iowa City, U.S.A.

B. Bilki[64], W. Clarida, K. Dilsiz[65], S. Durgut, R.P. Gandrajula, M. Haytmyradov, V. Khristenko, J.-P. Merlo, H. Mermerkaya[66], A. Mestvirishvili, A. Moeller, J. Nachtman, H. Ogul[67], Y. Onel, F. Ozok[68], A. Penzo, C. Snyder, E. Tiras, J. Wetzel, K. Yi

Johns Hopkins University, Baltimore, U.S.A.

B. Blumenfeld, A. Cocoros, N. Eminizer, D. Fehling, L. Feng, A.V. Gritsan, P. Maksimovic, J. Roskes, U. Sarica, M. Swartz, M. Xiao, C. You

The University of Kansas, Lawrence, U.S.A.

A. Al-bataineh, P. Baringer, A. Bean, S. Boren, J. Bowen, J. Castle, S. Khalil, A. Kropivnitskaya, D. Majumder, W. Mcbrayer, M. Murray, C. Royon, S. Sanders, E. Schmitz, J.D. Tapia Takaki, Q. Wang

Kansas State University, Manhattan, U.S.A.

A. Ivanov, K. Kaadze, Y. Maravin, A. Mohammadi, L.K. Saini, N. Skhirtladze

Lawrence Livermore National Laboratory, Livermore, U.S.A.

F. Rebassoo, D. Wright

University of Maryland, College Park, U.S.A.

C. Anelli, A. Baden, O. Baron, A. Belloni, S.C. Eno, Y. Feng, C. Ferraioli, N.J. Hadley, S. Jabeen, G.Y. Jeng, R.G. Kellogg, J. Kunkle, A.C. Mignerey, F. Ricci-Tam, Y.H. Shin, A. Skuja, S.C. Tonwar

Massachusetts Institute of Technology, Cambridge, U.S.A.

D. Abercrombie, B. Allen, V. Azzolini, R. Barbieri, A. Baty, R. Bi, S. Brandt, W. Busza, I.A. Cali, M. D'Alfonso, Z. Demiragli, G. Gomez Ceballos, M. Goncharov, D. Hsu, M. Hu, Y. Iiyama, G.M. Innocenti, M. Klute, D. Kovalskyi, Y.-J. Lee, A. Levin, P.D. Luckey, B. Maier, A.C. Marini, C. Mcginn, C. Mironov, S. Narayanan, X. Niu, C. Paus, C. Roland, G. Roland, J. Salfeld-Nebgen, G.S.F. Stephans, K. Tatar, D. Velicanu, J. Wang, T.W. Wang, B. Wyslouch

University of Minnesota, Minneapolis, U.S.A.

A.C. Benvenuti, R.M. Chatterjee, A. Evans, P. Hansen, J. Hiltbrand, S. Kalafut, Y. Kubota, Z. Lesko, J. Mans, S. Nourbakhsh, N. Ruckstuhl, R. Rusack, J. Turkewitz, M.A. Wadud

University of Mississippi, Oxford, U.S.A.

J.G. Acosta, S. Oliveros

JHEP09(2018)148

University of Nebraska-Lincoln, Lincoln, U.S.A.

E. Avdeeva, K. Bloom, D.R. Claes, C. Fangmeier, R. Gonzalez Suarez, R. Kamalieddin, I. Kravchenko, J. Monroy, J.E. Siado, G.R. Snow, B. Stieger

State University of New York at Buffalo, Buffalo, U.S.A.

J. Dolen, A. Godshalk, C. Harrington, I. Iashvili, D. Nguyen, A. Parker, S. Rappoccio, B. Roozbahani

Northeastern University, Boston, U.S.A.

G. Alverson, E. Barberis, C. Freer, A. Hortiangtham, A. Massironi, D.M. Morse, T. Orimoto, R. Teixeira De Lima, D. Trocino, T. Wamorkar, B. Wang, A. Wisecarver, D. Wood

Northwestern University, Evanston, U.S.A.

S. Bhattacharya, O. Charaf, K.A. Hahn, N. Mucia, N. Odell, M.H. Schmitt, K. Sung, M. Trovato, M. Velasco

University of Notre Dame, Notre Dame, U.S.A.

R. Bucci, N. Dev, M. Hildreth, K. Hurtado Anampa, C. Jessop, D.J. Karmgard, N. Kellams, K. Lannon, W. Li, N. Loukas, N. Marinelli, F. Meng, C. Mueller, Y. Musienko[35], M. Planer, A. Reinsvold, R. Ruchti, P. Siddireddy, G. Smith, S. Taroni, M. Wayne, A. Wightman, M. Wolf, A. Woodard

The Ohio State University, Columbus, U.S.A.

J. Alimena, L. Antonelli, B. Bylsma, L.S. Durkin, S. Flowers, B. Francis, A. Hart, C. Hill, W. Ji, B. Liu, W. Luo, B.L. Winer, H.W. Wulsin

Princeton University, Princeton, U.S.A.

S. Cooperstein, O. Driga, P. Elmer, J. Hardenbrook, P. Hebda, S. Higginbotham, A. Kalogeropoulos, D. Lange, J. Luo, D. Marlow, K. Mei, I. Ojalvo, J. Olsen, C. Palmer, P. Piroué, D. Stickland, C. Tully

University of Puerto Rico, Mayaguez, U.S.A.

S. Malik, S. Norberg

Purdue University, West Lafayette, U.S.A.

A. Barker, V.E. Barnes, S. Das, S. Folgueras, L. Gutay, M.K. Jha, M. Jones, A.W. Jung, A. Khatiwada, D.H. Miller, N. Neumeister, C.C. Peng, H. Qiu, J.F. Schulte, J. Sun, F. Wang, R. Xiao, W. Xie

Purdue University Northwest, Hammond, U.S.A.

T. Cheng, N. Parashar, J. Stupak

Rice University, Houston, U.S.A.

Z. Chen, K.M. Ecklund, S. Freed, F.J.M. Geurts, M. Guilbaud, M. Kilpatrick, W. Li, B. Michlin, B.P. Padley, J. Roberts, J. Rorie, W. Shi, Z. Tu, J. Zabel, A. Zhang

University of Rochester, Rochester, U.S.A.

A. Bodek, P. de Barbaro, R. Demina, Y.t. Duh, T. Ferbel, M. Galanti, A. Garcia-Bellido, J. Han, O. Hindrichs, A. Khukhunaishvili, K.H. Lo, P. Tan, M. Verzetti

JHEP09(2018)148

The Rockefeller University, New York, U.S.A.
R. Ciesielski, K. Goulianos, C. Mesropian

Rutgers, The State University of New Jersey, Piscataway, U.S.A.
A. Agapitos, J.P. Chou, Y. Gershtein, T.A. Gómez Espinosa, E. Halkiadakis, M. Heindl, E. Hughes, S. Kaplan, R. Kunnawalkam Elayavalli, S. Kyriacou, A. Lath, R. Montalvo, K. Nash, M. Osherson, H. Saka, S. Salur, S. Schnetzer, D. Sheffield, S. Somalwar, R. Stone, S. Thomas, P. Thomassen, M. Walker

University of Tennessee, Knoxville, U.S.A.
A.G. Delannoy, M. Foerster, J. Heideman, G. Riley, K. Rose, S. Spanier, K. Thapa

Texas A&M University, College Station, U.S.A.
O. Bouhali[69], A. Castaneda Hernandez[69], A. Celik, M. Dalchenko, M. De Mattia, A. Delgado, S. Dildick, R. Eusebi, J. Gilmore, T. Huang, T. Kamon[70], R. Mueller, Y. Pakhotin, R. Patel, A. Perloff, L. Perniè, D. Rathjens, A. Safonov, A. Tatarinov, K.A. Ulmer

Texas Tech University, Lubbock, U.S.A.
N. Akchurin, J. Damgov, F. De Guio, P.R. Dudero, J. Faulkner, E. Gurpinar, S. Kunori, K. Lamichhane, S.W. Lee, T. Libeiro, T. Mengke, S. Muthumuni, T. Peltola, S. Undleeb, I. Volobouev, Z. Wang

Vanderbilt University, Nashville, U.S.A.
S. Greene, A. Gurrola, R. Janjam, W. Johns, C. Maguire, A. Melo, H. Ni, K. Padeken, P. Sheldon, S. Tuo, J. Velkovska, Q. Xu

University of Virginia, Charlottesville, U.S.A.
M.W. Arenton, P. Barria, B. Cox, R. Hirosky, M. Joyce, A. Ledovskoy, H. Li, C. Neu, T. Sinthuprasith, Y. Wang, E. Wolfe, F. Xia

Wayne State University, Detroit, U.S.A.
R. Harr, P.E. Karchin, N. Poudyal, J. Sturdy, P. Thapa, S. Zaleski

University of Wisconsin - Madison, Madison, WI, U.S.A.
M. Brodski, J. Buchanan, C. Caillol, S. Dasu, L. Dodd, S. Duric, B. Gomber, M. Grothe, M. Herndon, A. Hervé, U. Hussain, P. Klabbers, A. Lanaro, A. Levine, K. Long, R. Loveless, T. Ruggles, A. Savin, N. Smith, W.H. Smith, D. Taylor, N. Woods

†: Deceased
1: Also at Vienna University of Technology, Vienna, Austria
2: Also at State Key Laboratory of Nuclear Physics and Technology; Peking University, Beijing, China
3: Also at IRFU; CEA; Université Paris-Saclay, Gif-sur-Yvette, France
4: Also at Universidade Estadual de Campinas, Campinas, Brazil
5: Also at Universidade Federal de Pelotas, Pelotas, Brazil
6: Also at Université Libre de Bruxelles, Bruxelles, Belgium
7: Also at Institute for Theoretical and Experimental Physics, Moscow, Russia
8: Also at Joint Institute for Nuclear Research, Dubna, Russia

JHEP09(2018)148

9: Now at Ain Shams University, Cairo, Egypt
10: Now at British University in Egypt, Cairo, Egypt
11: Also at Zewail City of Science and Technology, Zewail, Egypt
12: Also at Université de Haute Alsace, Mulhouse, France
13: Also at Skobeltsyn Institute of Nuclear Physics; Lomonosov Moscow State University, Moscow, Russia
14: Also at CERN; European Organization for Nuclear Research, Geneva, Switzerland
15: Also at RWTH Aachen University; III. Physikalisches Institut A, Aachen, Germany
16: Also at University of Hamburg, Hamburg, Germany
17: Also at Brandenburg University of Technology, Cottbus, Germany
18: Also at MTA-ELTE Lendület CMS Particle and Nuclear Physics Group; Eötvös Loránd University, Budapest, Hungary
19: Also at Institute of Nuclear Research ATOMKI, Debrecen, Hungary
20: Also at Institute of Physics; University of Debrecen, Debrecen, Hungary
21: Also at Indian Institute of Technology Bhubaneswar, Bhubaneswar, India
22: Also at Institute of Physics, Bhubaneswar, India
23: Also at University of Visva-Bharati, Santiniketan, India
24: Also at University of Ruhuna, Matara, Sri Lanka
25: Also at Isfahan University of Technology, Isfahan, Iran
26: Also at Yazd University, Yazd, Iran
27: Also at Plasma Physics Research Center; Science and Research Branch; Islamic Azad University, Tehran, Iran
28: Also at Università degli Studi di Siena, Siena, Italy
29: Also at INFN Sezione di Milano-Bicocca; Università di Milano-Bicocca, Milano, Italy
30: Also at Purdue University, West Lafayette, U.S.A.
31: Also at International Islamic University of Malaysia, Kuala Lumpur, Malaysia
32: Also at Malaysian Nuclear Agency; MOSTI, Kajang, Malaysia
33: Also at Consejo Nacional de Ciencia y Tecnología, Mexico city, Mexico
34: Also at Warsaw University of Technology; Institute of Electronic Systems, Warsaw, Poland
35: Also at Institute for Nuclear Research, Moscow, Russia
36: Now at National Research Nuclear University 'Moscow Engineering Physics Institute' (MEPhI), Moscow, Russia
37: Also at St. Petersburg State Polytechnical University, St. Petersburg, Russia
38: Also at University of Florida, Gainesville, U.S.A.
39: Also at P.N. Lebedev Physical Institute, Moscow, Russia
40: Also at California Institute of Technology, Pasadena, U.S.A.
41: Also at Budker Institute of Nuclear Physics, Novosibirsk, Russia
42: Also at Faculty of Physics; University of Belgrade, Belgrade, Serbia
43: Also at University of Belgrade; Faculty of Physics and Vinca Institute of Nuclear Sciences, Belgrade, Serbia
44: Also at Scuola Normale e Sezione dell'INFN, Pisa, Italy
45: Also at National and Kapodistrian University of Athens, Athens, Greece
46: Also at Riga Technical University, Riga, Latvia
47: Also at Universität Zürich, Zurich, Switzerland
48: Also at Stefan Meyer Institute for Subatomic Physics (SMI), Vienna, Austria
49: Also at Istanbul Aydin University, Istanbul, Turkey
50: Also at Mersin University, Mersin, Turkey
51: Also at Cag University, Mersin, Turkey

JHEP09(2018)148

52: Also at Piri Reis University, Istanbul, Turkey
53: Also at Gaziosmanpasa University, Tokat, Turkey
54: Also at Adiyaman University, Adiyaman, Turkey
55: Also at Izmir Institute of Technology, Izmir, Turkey
56: Also at Necmettin Erbakan University, Konya, Turkey
57: Also at Marmara University, Istanbul, Turkey
58: Also at Kafkas University, Kars, Turkey
59: Also at Istanbul Bilgi University, Istanbul, Turkey
60: Also at Rutherford Appleton Laboratory, Didcot, United Kingdom
61: Also at School of Physics and Astronomy; University of Southampton, Southampton, United Kingdom
62: Also at Instituto de Astrofísica de Canarias, La Laguna, Spain
63: Also at Utah Valley University, Orem, U.S.A.
64: Also at Beykent University, Istanbul, Turkey
65: Also at Bingol University, Bingol, Turkey
66: Also at Erzincan University, Erzincan, Turkey
67: Also at Sinop University, Sinop, Turkey
68: Also at Mimar Sinan University; Istanbul, Istanbul, Turkey
69: Also at Texas A&M University at Qatar, Doha, Qatar
70: Also at Kyungpook National University, Daegu, Korea

JHEP09(2018)148